HIGH RESOLUTION HABITAT SUITABILITY MODELING FOR A NARROW-RANGE ENDEMIC ALPINE HAWAIIAN SPECIES

A THESIS SUBMITTED TO THE GRADUATE DIVISION OF THE UNIVERSITY OF HAWAIʻI AT HILO IN PARTIAL FULFILLMENT OF THE REQUIREMENTS FOR THE DEGREE OF

MASTER OF SCIENCE
IN
TROPICAL CONSERVATION BIOLOGY AND ENVIRONMENTAL SCIENCE

MAY 2016

By: Nathan Michael Stephenson

Thesis Committee:

Ryan Perroy, Chairperson
Jesse Eiben
Frederick Klasner

Keywords: Microhabitat, Structure from Motion, Lidar, MaxEnt, Habitat Suitability

ACKNOWLEDGMENTS

I would like to thank the Office of Maunakea Management for funding this project and also providing vehicles and equipment when necessary. The Office of Maunakea Management has been instrumental in the completion of this project and is a great resource for the community, with knowledgeable staff and access to information. I would also like to thank UNAVCO for facilitating the collection of high resolution lidar data and providing us with an excellent analyst, Marianne Okal. I would like to thank the Pacific Internship Programs for Exploring Science (PIPES) which provided a brilliant summer intern, Sean Kirkpatrick, who was a pleasure to work with.

I would like to give a special thanks to my graduate committee Ryan, Frederick, and Jesse. Ryan has been an incredible teacher and mentor for my undergraduate and graduate careers and the completion of this project would not have been possible without his continued guidance and support. Frederick, Fritz, has facilitated and participated in many field collections and directed me to the resources and information necessary to finish this thesis. Jesse has been an invaluable resource with a wealth of knowledge about the Maunakea summit and our species of interest. Jesse is also a riot to work with in the field. I would also like to thank the many people that have helped me along this journey, whether it be with field work, data processing, or moral support:

-SILVANA CARES
-JESSICA KIRKPATRICK
-AMBER STILLMAN
-DARCY YOGI
-NICK TURNER
-JORDEN ZARDERS
-HEATHER STEVER
-HEATHER KIMBALL
-KEN HON
-JONATHAN KOCH
-STEVE LUNDBLAD
-MOM
-DAD

ABSTRACT

Mapping potentially suitable habitat is critical for effective species conservation and management but can be challenging in remote areas exhibiting complex substrate heterogeneity. An approach that combines a diverse set of nonintrusive spatial data collection techniques with field validation can lead to a better understanding of landscapes and species distributions. *Nysius wekiuicola,* commonly known as the wēkiu bug, is the most studied arthropod species endemic to the Maunakea summit in Hawai‘i, yet details of its life history and geographic distribution remain poorly understood. The wēkiu bug, a species of concern, provides an excellent opportunity to employ nonintrusive spatial data collection techniques to answer previously elusive questions about habitat quality and composition. To predict the geographic distribution of *N. wekiuicola*, MaxEnt habitat suitability models were generated from fifteen years of species occurrence data and a variety of spatial datasets, including high resolution digital elevation models, surface mineralogy based on hyperspectral remote sensing, and climate variables. MaxEnt model results indicate that the variables with the highest influence (in terms of percent contribution) were elevation (78.2%), presence of nanocrystalline hematite surface minerals (13.7%), and minor contributions from aspect, slope, and other surface minerals. A limitation of this study is that many historic trapping sites were placed near roads and other accessible pre-determined locations instead of being systematically or randomly placed, meaning final model results may be biased and not entirely indicative of true wēkiu bug distribution. Although climate data is available, these climatic variables were auto-correlated and at too coarse of a spatial resolution to include in the final analysis. A trapping experiment based on surface mineralogy and geomorphic position affirmed that both elevation and surface mineralogy play significant roles in the spatial patterns of wēkiu bugs, but observed presence upslope on a cinder cone and absence downslope, even within the same predominant surface mineral, suggests that other habitat variables may be at play such as competition/predation. The models of wēkiu bug range and predicted suitable locations will be incorporated into management efforts and restoration goals for land managers of Maunakea. In addition, environmental data layers created in this initiative have now unlocked the ability to create suitability models for other species of interest on Maunakea.

TABLE OF CONTENTS

LIST OF TABLES

LIST OF FIGURES

INTRODUCTION

Typical conservation management actions for at-risk species may include fencing programs in degraded areas (Cabin *et al.* 2000), captive rearing and reintroduction (Reed *et al.* 2012), and prevention or eradication of harmful invasive species (Burnett *et al*. 2006). But land managers may only have limited existing knowledge of key environmental habitat variables and total species geographic distributions that could better inform management decisions. Habitat models that identify current areas of suitability and define important ecogeographical variables can improve management of a focal species and better manage possible threats (Hirzel *et al.* 2002; Thuiller & Munkemuller, 2010; Franklin, 2010). Habitat suitability modeling has proven difficult for species that live in remote and challenging ecosystems that lack accurate high resolution datasets (Peterson & Nakazawa, 2008). Heterogeneous intertidal seagrass (Hannam & Moskal, 2015) and invasive plants in tropical rainforests (Asner *et al.* 2008) represent seemingly difficult to map species and environments that have been quickly and successfully mapped with minimal habitat intrusion using spatial technologies including laser scanning and/or imaging spectroscopy. These and other technologies can be used to rapidly collect data and generate the habitat variable datasets necessary for suitability modeling. The wēkiu bug *Nysius wekiuicola* (Ashlock & Gagne, 1983), endemic to the upper summit (3350-4205 m) region of the post shield volcano Maunakea, represents a species where information regarding important habitat variables predictive of its geographic range has been scarce, and would benefit from non-intrusive detailed mapping techniques.

The flightless wēkiu bug resides in a geographically small area of alpine stone desert on the summit of Maunakea, the tallest of five volcanoes on Hawai‘i Island (Figure 1). Maunakea topography was formed by late stage volcanism and at least three glaciation episodes (Porter, 2005), the last of which was 13-40,000 years ago (Wolfe *et al.* 1997) which created a complex of steep irregular cinder cones, glacial moraines, erosional features, hydrothermally altered basaltic tephra (Morris *et al.* 2000), and glacial scour and lava flows (Wolfe & Morris, 1996). Much of the summit is remote, requiring permits for data collection, and is also an important aeolian ecosystem that contains numerous cultural resources and species of concern (Juvik & Juvik, 1984; McCoy, 1976; Stemmermann, 1989; Eiben & Rubinoff, 2010). In addition, summit cinder

cones are mainly composed of loosely packed rock tephra that can be easily damaged or degraded (Richardson, 2002). For these reasons, the Maunakea summit and endemic wēkiu bug represent an intriguing place and species where non-intrusive spatial data gathering techniques can be effectively applied to generate data, create habitat suitability models and define important habitat variables.

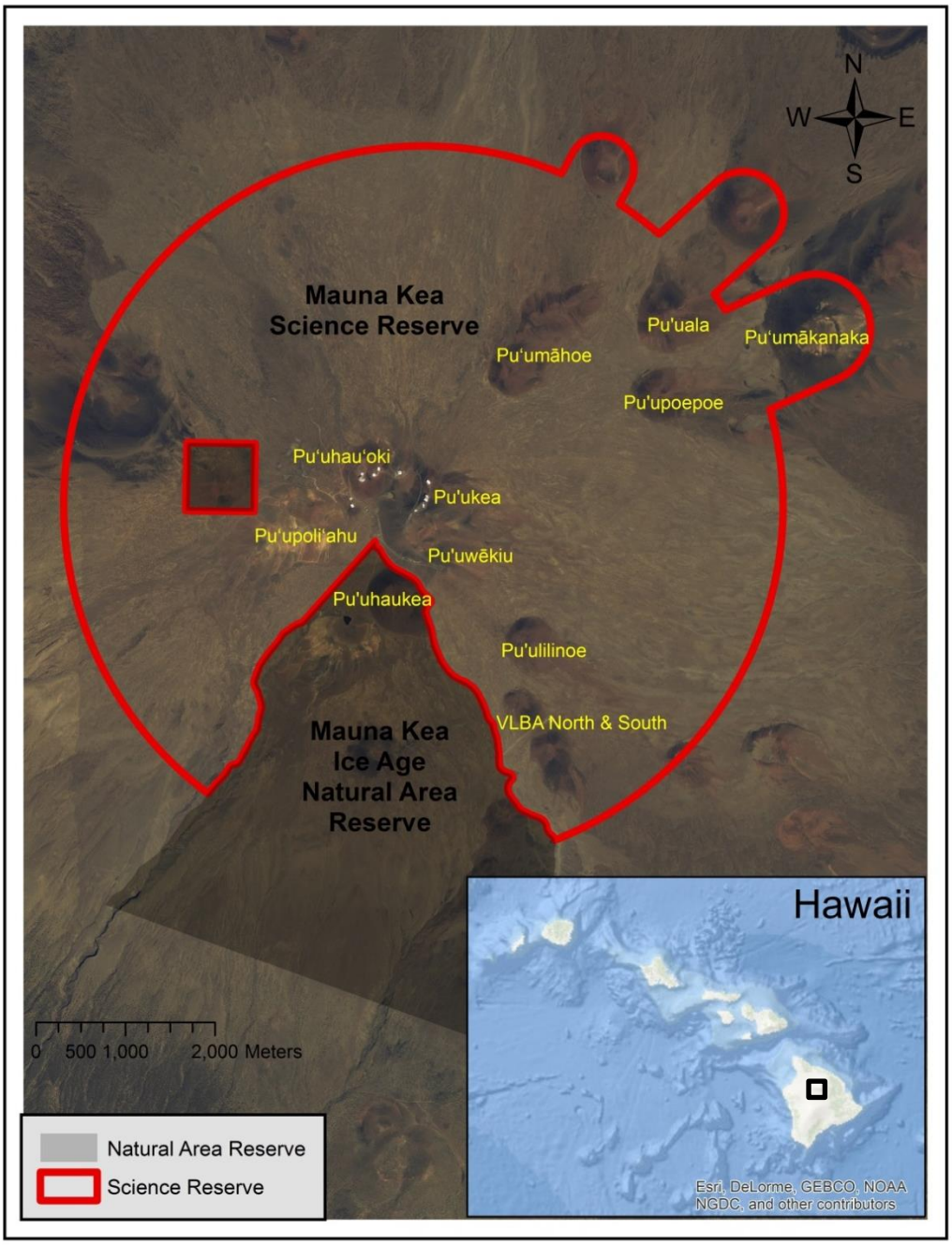

Figure 1: Maunakea summit consisting of the Mauna Kea Science Reserve (UH), Natural Area Reserve, Astronomy Precinct (DLNR) (not labelled) and a number of Pu‘u or cinder cones. The summit also contains the world’s most advanced ground-based constellation of 13 astronomy telescopes. Inset map shows the general location of the summit on Hawai‘i Island.

Although first discovered in 1979 (Howarth & Montgomery, 1980) and studied for over 35 years, questions remain regarding wēkiu bug life history characteristics, potential threats to species persistence, geographic range and suitable habitat. Previous hypotheses have suggested that wēkiu bug habitat consists mainly of the crater rims of cinder cones that were not overtopped by glaciers (nunataks) and north or east facing slopes where local topography causes snowpack to persist longer on average (Porter & Englund, 2006). Wēkiu bug habitat has also been described as loose porous scoria/tephra (Eiben & Rubinoff, 2010) ranging in size from fine ash to 10 cm, with optimal tephra size being 1-5 cm on certain cinder cones (Brenner, 2005). This rock tephra layer is hypothesized to act as a thermal buffer allowing for adequate thermoregulation and sufficient cover from predation (Eiben & Rubinoff, 2014). Temperatures recorded at the surface of this rock tephra layer can vary drastically up to 46^{o}C during the day and -15^{o}C at night, with a much smaller range of temperature fluctuation into the ash layer. Similarly, relative humidity can fluctuate considerably between the rock surface and into the ash layer (Eiben & Rubinoff, 2010). Tephra deposits also contain various vesicle sizes and densities that are related to glacial and post-glacial volcanic activity (Wolfe *et al.* 1997). These deposits underwent alteration phase changes during and post-emplacement from Hawaiite basaltic tephra to various other surface minerals (Swayze & Hon, Personal Communication, 2016). The spatial patterns of these surface mineral alterations may also play a part in the successful captures of wēkiu bugs. Many of these definitions based on informal observations and correlations to ex-situ studies, remain somewhat speculative.

The upper summit was previously classified into six arthropod habitat types, one of which was considered highly suitable for wēkiu bugs: tephra ridges or slopes; three considered marginal: snow patches, loose tephra slopes, and talus or fractured rock outcrops; and two considered unsuitable or uncommonly found in: lava flows and ash/silt (TMT EIS, 2010, Section 3.4). Entire cinder cone/complexes have been considered broadly suitable habitat in the past without verification of the environmental variables associated with successful captures. This is problematic because failing to identify habitat variables associated with successful captures means we cannot extrapolate to other areas have that have not been fully sampled. Also, cinder cones may not be homogenously suitable, but could instead contain suitable microhabitats within broadly defined cinder cones. Using these previous definitions, possible ecogeographical habitat variables that influence wēkiu bug geographic distribution may include topographic variables

(elevation, aspect, slope, surface roughness, and geomorphic position), surface mineralogy, depth to the underlying ash layer or finest scale material (related to eruptive processes which bore non-uniform depths across the summit), climate variables (solar radiation, surface temperature, rainfall, relative humidity, actual evapotranspiration, and latent heat flux) and food and water availability. The combination of surface mineralogy and certain climate variables may also be related to the way rock tephra heats and cools, which affect wēkiu bug growth cycles and movement potential.

The aim of this study is to model the range of suitable wēkiu bug habitat and define important habitat variables that can account for the patterns of previous capture data. This will serve to improve existing management practices, remodel future sampling patterns and help guide restoration efforts. In order to model the geographic range and identify important habitat variables we compiled a wide variety of datasets including wēkiu bug presence data, surface mineralogy, high resolution topography generated from terrestrial lidar and unmanned aerial vehicles (UAVs), climate variables, and created suitability models using MaxEnt (Phillips *et al.* 2006).

MATERIALS AND METHODS

MaxEnt is a statistical software program that uses ecogeographical habitat variables and occurrence data to model a species geographic range (Elith et al. 2010). MaxEnt has been widely used across the globe to successfully model species of concern (Kumar & Stohlgren, 2009; Weinsheimer *et al*. 2010; Magris & Destro, 2010; Manthey *et al*. 2015). MaxEnt has an intuitive graphical user interface and is widely used, referenced in over 1000 publications since 2006 (Merow et al. 2013). In comparison studies for MaxEnt and other habitat suitability modeling software packages such as GARP, Bioclim and Domain, MaxEnt generally produces the strongest results and highest accuracies (Hernandes et al. 2006). MaxEnt has also been used for both broad- and fine-scale habitat suitability modeling (Razgour et al. 2011). For these reasons, MaxEnt was chosen over other suitability modeling software. In order to model the geographic range and suitable habitat for wēkiu bugs, different habitat variables must be available (compiled or generated) at the same geographic extent and spatial resolution. Here we describe the different datasets included in the model and how they were collected.

Topographic Terrain Characterization

In order to characterize terrain at the summit of Maunakea we generated a high resolution topographic dataset using a VZ-1000 Riegl terrestrial survey grade lidar scanner (TLS) with a Nikon D800 mounted camera with a 1400 m scanning range. We collected TLS data at 94 locations (Figure 2) producing point clouds (33 pts/m^2 average) using RiSCAN PRO over ~15 km^2 from August 19-28th, 2014. Lidar scanning positions were setup no more than 800-1000 m from summit access roads for safety and efficiency. In order to limit scaling errors due to atmospheric conditions temperature, relative humidity, and air pressure values were collected using a Kestrel 4000 Weather Monitor and supplied to the TLS to calculate a scaling adjustment factor. TLS data were merged and aligned using 16.5 cm diameter red targets systematically placed in the environment which served as tie points between scanning positions. Data were georeferenced using Earth-Centered, Earth-Fixed Cartesian coordinates gathered from International GNSS Service, NASA Jet Propulsion Laboratory operated differential GPS base

station MKEA. A total of 71 target positions were occupied for >thirty minutes, and seventeen scanner positions occupied for >twenty minutes by UNAVCO (Okal, 2016; unavco.org). The resulting dataset included a nearly continuous point cloud of a portion the study region. Raw lidar point clouds were processed into digital elevation models (DEMs) in LAStools (rapidlasso, 2015) with a cell size of 1 m.

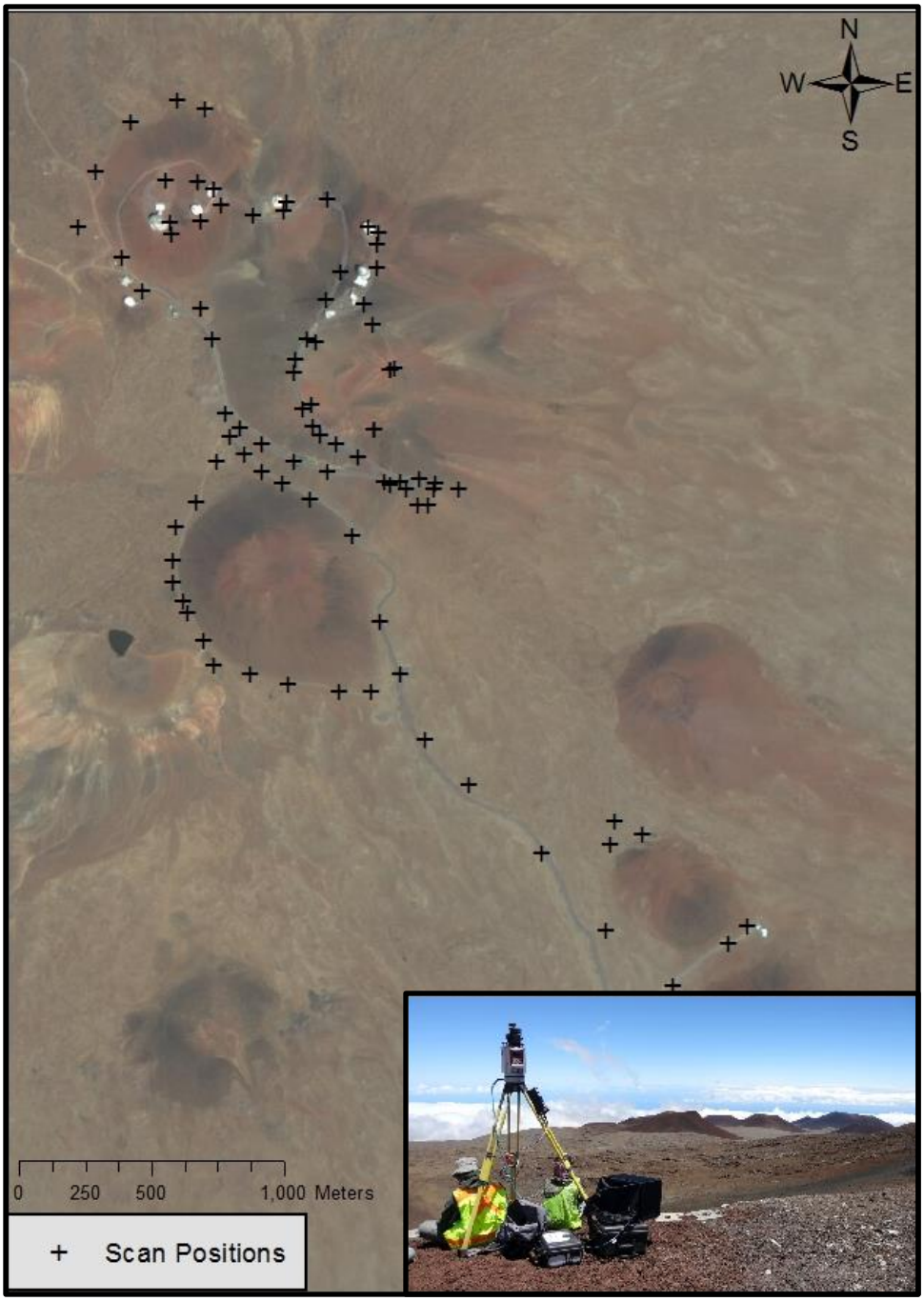

Figure 2: 94 TLS data collection locations focusing on the summit cinder cone complex, which has been the historical wēkiu bug population center. Inset: typical TLS setup overlooking a distant cinder cone complex.

Inclement weather was encountered on August 21st with high wind conditions 10-15 knots with 15 knot gusts, and on August 28th with foggy conditions while conducting lidar scans. Data points collected on August 28th were filtered and all fog-related erroneous points were excluded from the final dataset to limit any errors while generating DEMs. High wind conditions may cause the TLS to vibrate during data collection which causes irreversible errors. These errors are much more difficult to assess and cannot be filtered.

Lidar data may contain occlusions due to environmental obstacles and perspective issues for which no data points will be present (Perroy *et al.*, 2010; Leslar, 2015). Our 2014 TLS dataset contained multiple occlusions caused by cinder cones with convex craters and areas difficult to access, impeding the calculation of habitat variables in ~100 trapping locations. To 'fill' two important occlusions (36,081 m^2 within the interior crater of a cinder cone and 256,485 m^2 exterior portion of another remote cone) new topographic datasets were created via Structure from Motion (SfM) by taking photos of the missing area from ground and UAV camera campaigns. A Nikon D7100 DSLR camera were used to collect terrestrial photos and a DJI Inspire 1 Pro with a wide-angle rectilinear lens, 4K video camera mounted on a ZENMUSE X3 advanced gimbal were used to collect high definition videos from which still images were extracted. Ground based photos of the interior crater used three tie points, occupied for >fifteen minutes with a Trimble XH 6000. Aerial UAV photos of the remote cone's eastern flank used nine tie points, occupied for >five minutes with a Trimble XH 6000. Geographic coordinates occupied at each tie point were differentially corrected in GPS Pathfinder Office using GPS base station MKEA. Images were then processed into point clouds using PIX4D 2.1. The combination of SfM and lidar data has proven effective at increasing both horizontal and vertical accuracies and limiting the number of final occlusions in datasets (Chen et al. 2004; Wood & Mohammadi) but image blur caused by movement of the UAV during image capturing can cause errors if blurred images are not removed before generating DEMs (Rhee & Kim, 2015). Blurred images were identified and excluded during the generation of point clouds.

DEMs generated from SfM data had vertical errors that were generally higher for the ground-based photo campaign than for the UAV survey ranging between +3.76 and -1.75 m in comparison to the TLS data. The overall average error was calculated and a correction factor applied resulting in <0.05 m final error for both datasets. CloudCompare 2.6.3 was used to merge

SfM data and TLS data into a single point cloud dataset. LAStools was used to process point clouds into continuous DEMs (1 m cell size) from which slope, aspect (Figure 3) and surface roughness approximations (not shown) were derived.

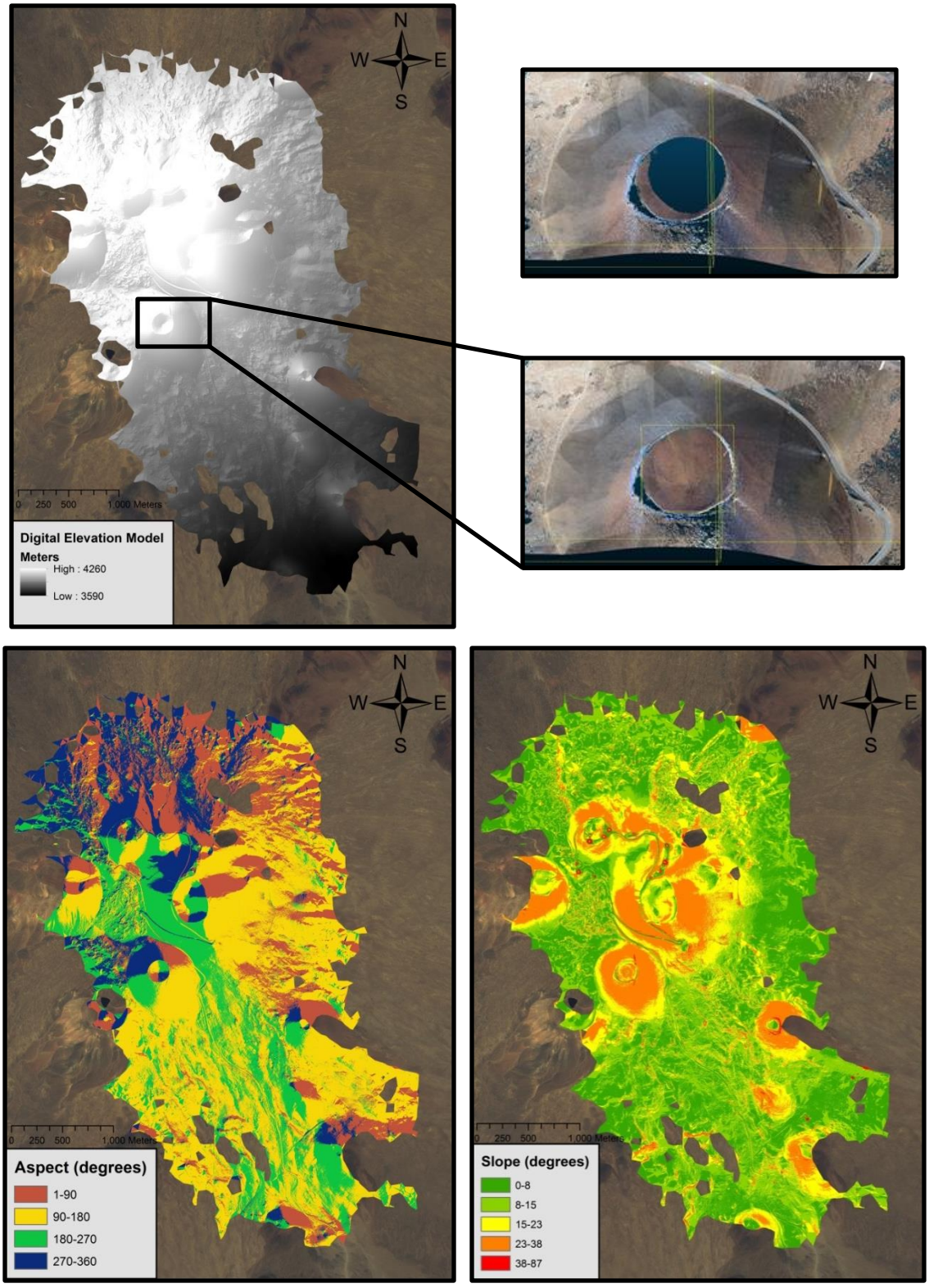

Figure 3: DEM (upper left) generated from TLS data and certain derivatives aspect (lower left) and slope (lower right), both in degrees. Upper right displays one of the occlusions which was filled with SfM (location outlined in black box). These datasets cover approximately 15 km^2.

During the 2015 Office of Maunakea Management (OMKM) annual arthropod survey 71 locations (see appendix Table 7) were measured for depth to the underlying ash layer and tephra gradation, which is the natural sorting of rocks, in addition to the placement of live-baited arthropod traps. This was done so depth to the ash layer and tephra gradation could be directly compared with wēkiu bug capture data. Depth measurements were made by creating a plane from the top rock layer and excavating a small hole until reaching the ash layer (or finest sediment layer). Tephra gradation from the surface to the ash/silt layer was recorded as normal (large rocks to smaller rocks), reverse (small rocks to larger rocks) or none (single rock sizes without an obvious gradation). After measurements were taken a live-baited pitfall trap was placed in the excavated pit and left for three days. Thirty-two additional depth and tephra gradation measurements were collected alone without trapping data (Figure 4) to better understand depth to the ash layer spatially across the summit. Certain areas of summit cinder cones have extreme slopes and loose material and could not be sampled.

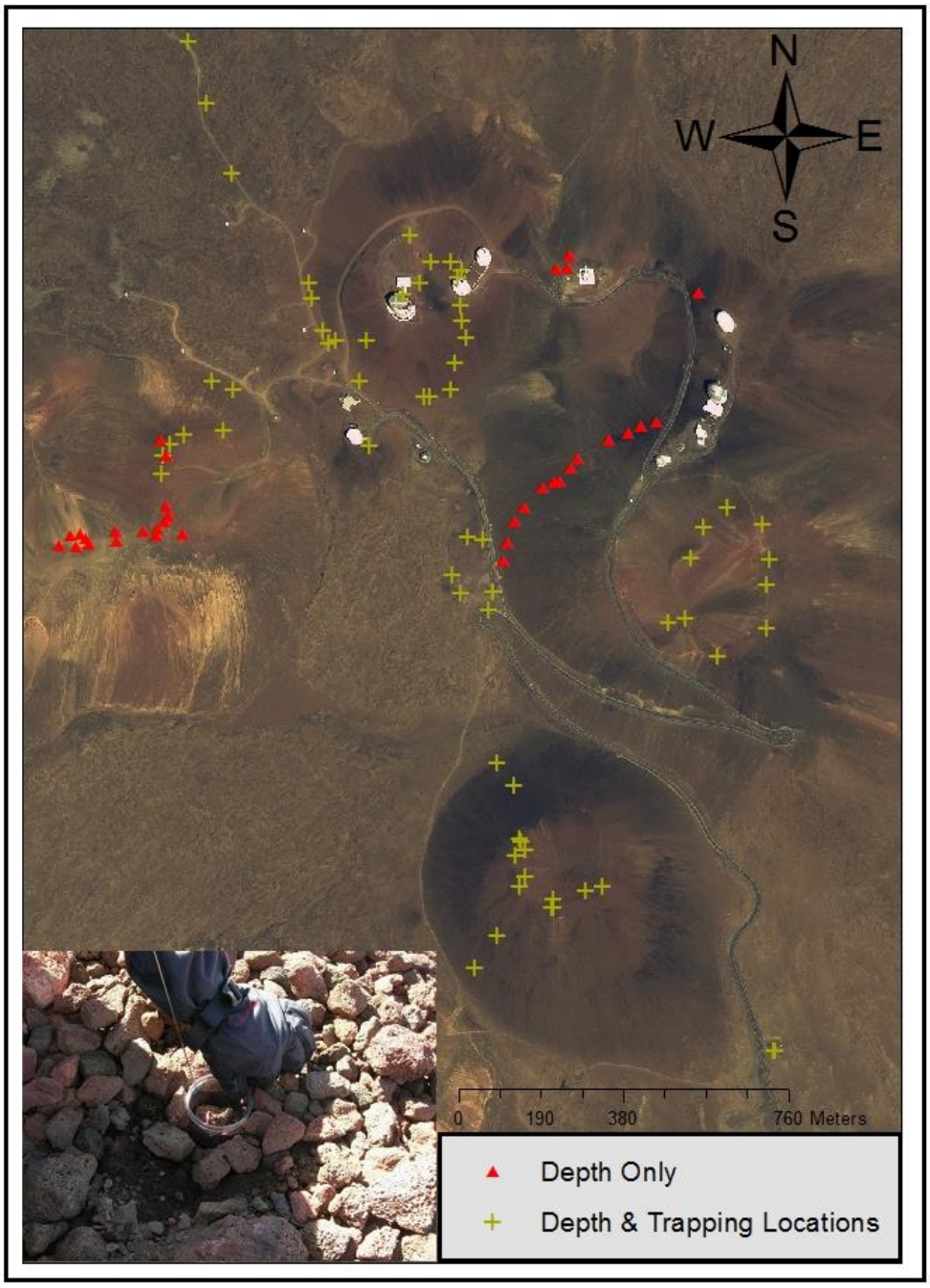

Figure 4: A subset of 2015 trapping locations where depth measurements were also recorded in cm (plus symbol) and depth only locations (red triangle) across a portion of summit. Inset map shows the placement of a live-baited arthropod trap flush with the rock surface layer.

Mineral Characterization

To characterize surface mineralogy, an existing hyperspectral AVIRIS-derived 20 m resolution electronic region (0.4 -1.35µm) mineralogy map was obtained of the study area (Swayze et al. 2002). Predominant surface minerals included nanocrystalline hematite, hematite, goethite, glassy volcanic rock, Fe 2+ minerals, amorphous Fe- hydroxides, and weathered Fe 2+ minerals. Geographic coordinates were assigned to this non-georeferenced classification through an image to image co-registration process in ENVI 5.3, using WorldView 2 satellite imagery as the base image file.

The resolution of the original mineral classification (20 m) was too coarse to accurately represent the variability and detail across the summit. A classification workflow was followed to create a new, higher resolution surface mineralogy map (Figure 5). Training regions were selected in 112 total areas representative of each mineral class and applied to a multiband WorldView 2 satellite image. Training regions were used to run a maximum likelihood classification (Richards, 1999) in ENVI 5.3 creating a 0.5 m spatial resolution surface mineralogy map (Figure 6). Nanocrystalline hematite and hematite were combined into a single mineral class: hematite. A Majority/Minority filtering technique was used to clean spurious pixels. Data were resampled to have the same pixel resolutions as lidar data (1 m). The high resolution lidar dataset covered >15 km^2 but it did not cover the know distribution of wēkiu bugs and ancillary coarser resolution 10 m data (Department of Commerce, 2007) were needed to supplement areas without high resolution data. Surface mineralogy classification was also resampled to 10 m to have the same pixel resolution as the 10 m data.

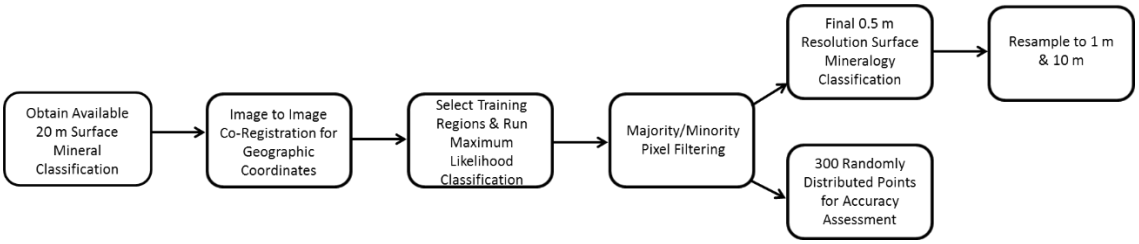

Figure 5: Model-building chart showing the workflow used to generate the final surface mineralogy classification and resampled data products.

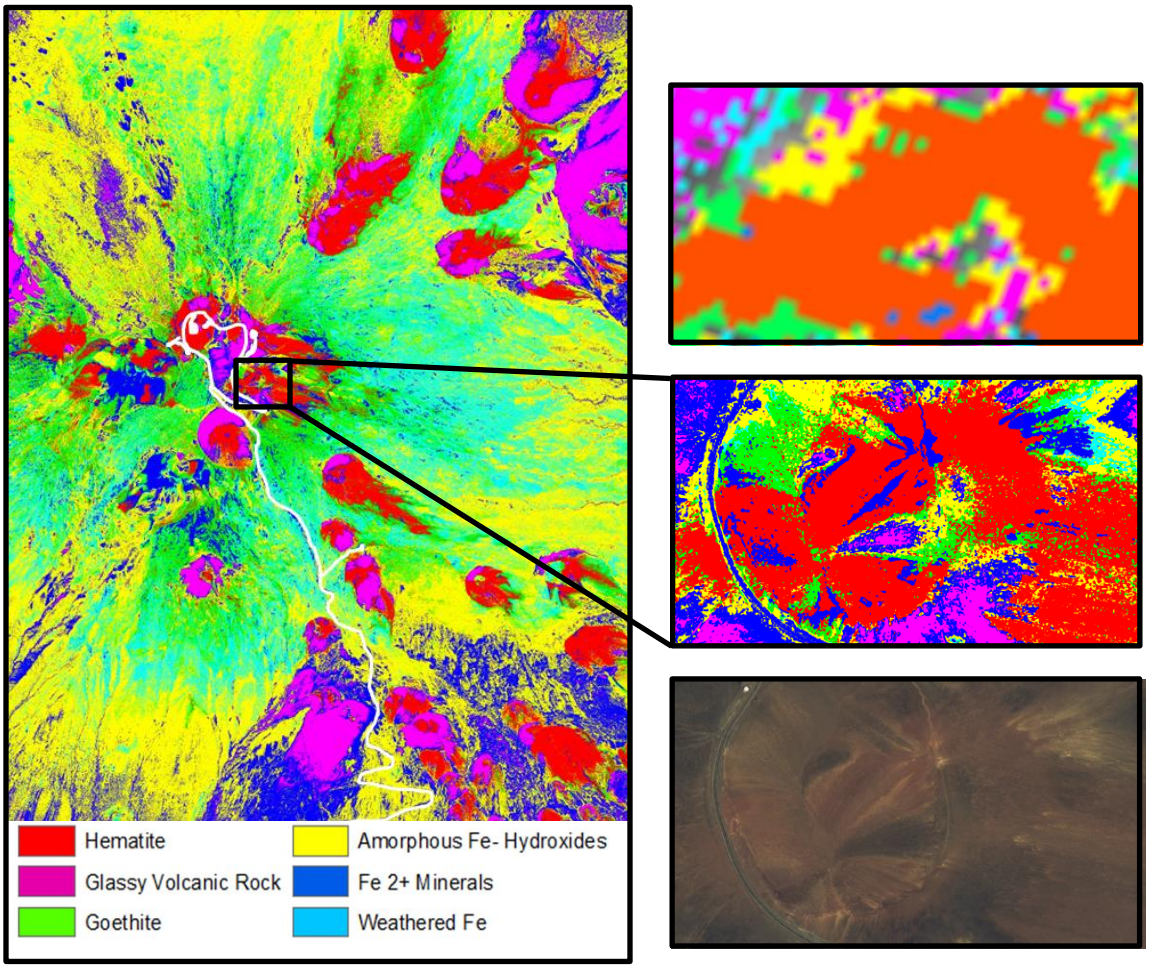

Figure 6: 0.5 m resolution surface mineralogy classification detailing the spatial patterns for six predominant surface minerals across the study area (left), inset images show the original 20 m classification (upper right), our new 0.5 m classification (middle right) and 2014 WorldView 2 satellite data (lower right).

The new 0.5 m resolution surface mineralogy classification shows that generally, summit cinder cones are composed of altered hematite and glassy volcanic rock, while previously glaciated areas are composed of the remaining four mineral types. Summit access roads and structures were masked out of the final classification. Accuracy assessment was performed using 300 randomly distributed points across the study area generated in ArcMap 10.3. Mineral class values at each point were assessed using 0.5 m WorldView 2 satellite imagery and a confusion matrix generated to test classification accuracy (Table 1). For accuracy assessment purposes, hematite and glassy volcanic rock were considered distinct classes while the remaining four mineral were merged into a single class. Overall classification accuracy achieved was 96.7% with a 0.85 Kappa statistic. Glassy volcanic rock and hematite received accuracies of 86.67% & 85.71%, respectively. Previous hypotheses suggested that wēkiu bugs were restricted to cinder cones (Porter & Englund, 2006), which according to this mineral classification are composed mainly of hematite and glassy volcanic rock (aside from Puʻupoliʻahu and Puʻuwaiau). We hypothesized that hematite and glassy volcanic rock minerals on cinder cones represent a higher degree of suitable habitat than on a cinder cone toe or in surrounding glacial till/lava flow areas with other surface minerals.

Table 1: Confusion matrix results from a manual accuracy assessment testing classification accuracy.

	Hematite	Glassy Volcanic Rock	Other Minerals	Total	User's Accuracy
Hematite	18.00	0.00	3.00	21.00	85.71
Glassy Volcanic Rock	0.00	13.00	2.00	15.00	86.67
Other Minerals	3.00	2.00	262.00	267.00	98.13
Total	21.00	15.00	267.00	303.00	
Producer's Accuracy	85.71	86.67			
Total Accuracy	96.70				
Kappa	0.85				

To verify that mineral classes in the new 0.5 m resolution surface mineralogy classification were spectrally distinct 29 surface mineral samples were collected across the study area representing all six predominant mineral types. The samples were analyzed using an analytical spectral device (ASD) Field Spectroradiometer Jr. with a 350-2500 nm spectral range and 10 nm spectral resolution. All samples were analyzed under laboratory conditions (Figure 7) using an illuminator reflectance lamp and bare fiber optic cable over black sample plates. Optimization and dark current readings were taken to accommodate specific lighting conditions.

Calibrations were performed between samples using a Spectralon panel and raw data were converted to reflectance. ASD results (Figure 8) confirmed that each mineral class had distinct spectral signatures.

Figure 7: ASD FieldSpec lab setup using a reflectance lamp for illumination and Spectralon standard between each mineral sample to maximize spectra signals.

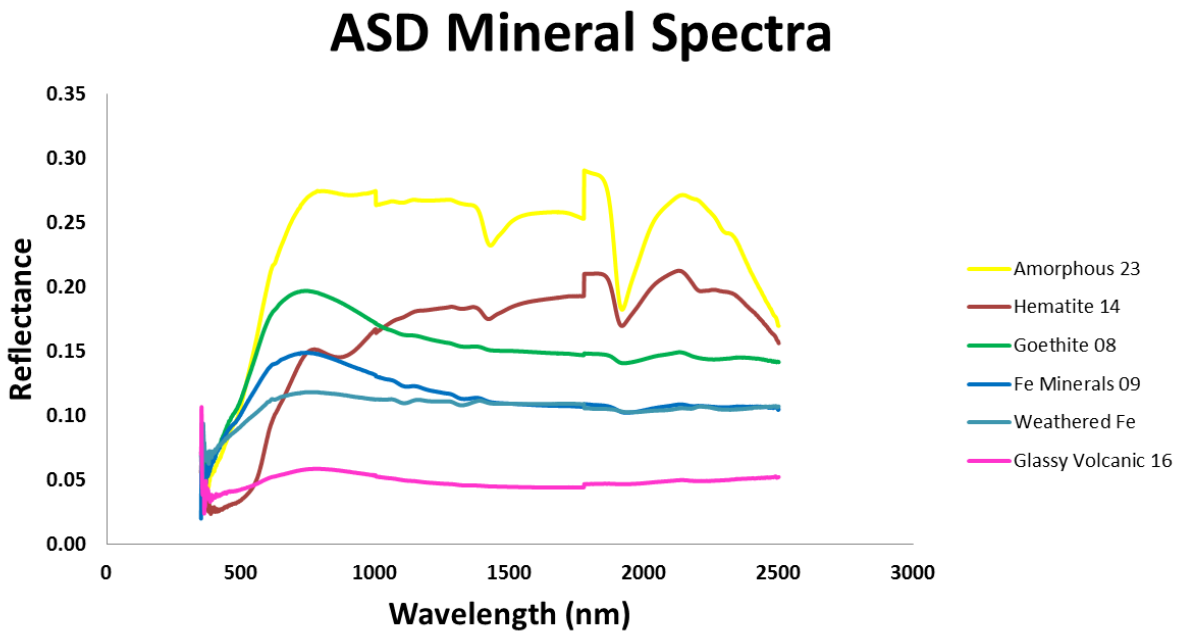

Figure 8: ASD data converted into reflectance for six different samples shows that each mineral type has a distinct spectral signature. Reflectance drops near 1800 nm due to moisture content in some of the samples. The abrupt vertical increase in reflectance near 2000 nm for some samples is an offset error with the ASD Fieldspec.

Although mineral classes displayed distinct spectral signatures we also wanted to test elemental compositions for a better understanding of mineralogy. In order to nondestructively quantify elemental composition a Thermo Scientific ARL Quant'XTM Energy Dispersive X-ray Fluorescence (ED XRF) were used. ED XRF uses a Rhodium stable-isotope X-ray tube, silicon drift detector, and Edmunds vacuum pump to measure composition from twenty elements. Wintrace 7.2 software was used to analyze elemental data. Powdered standards were formed into pellets using 2% polyvinyl alcohol binder and pressed using a 25-ton hydraulic press. Standards were then used to calibrate the ED XRF to maximize elemental concentration accuracy in samples (Lundblad *et al*. 2008; Lundblad *et al.* 2011). ED XRF analysis of whole rock samples representative of each mineral sample showed non-distinct elemental compositions between mineral types for elements such as Fe (Figure 9) and MgO, SiO2, K2O, CaO, TiO2, Cr, Ni, Cu, Zn, Rb, Sr, Y, Nb, Ba (not shown) and moderate elemental compositional differences between Na2O, Al2O3, V & MnO (Table 2).

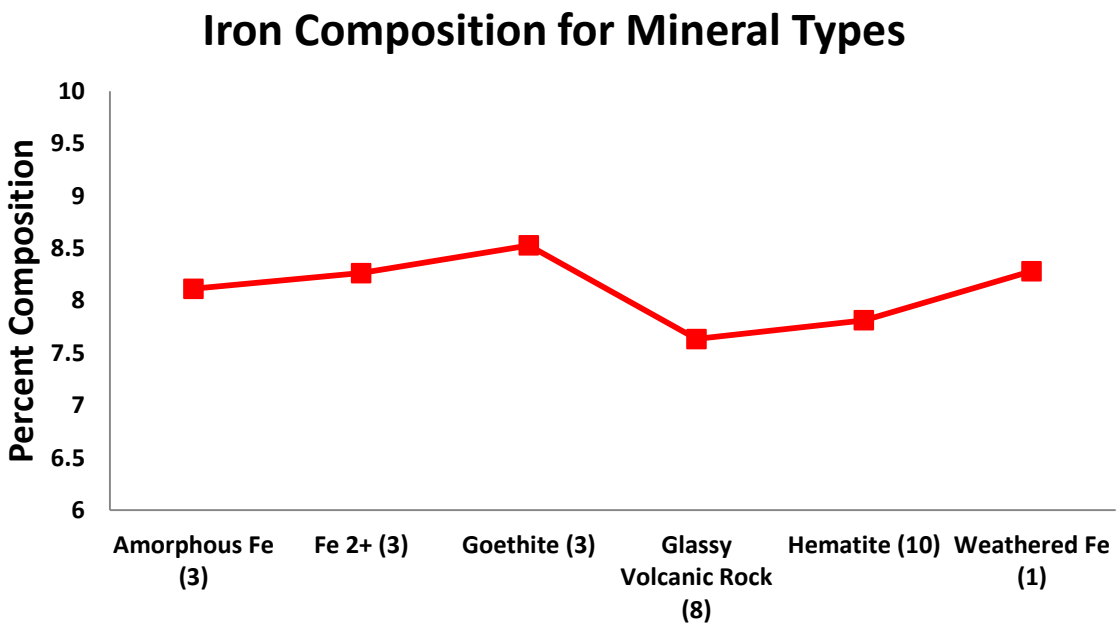

Figure 9: Fe elemental composition averages from all samples in each mineral class gathered from ED XRF analysis. Fe % composition varies little between mineral types. Parenthesis indicates the number of total samples used to calculate average values.

Table 2: Elemental composition averaged for all mineral samples shows slight difference for certain elements. * indicates values that are in parts per million

	Na_2O	StDEV	Al_2O_3	StDEV	V*	StDEV	MnO*	StDEV	Zr*	StDEV
Amorphous Fe (3)	1.26%	0.39	11.18%	2.03	103.89	29.06	2975.32	842.30	541.84	43.04
Fe 2+ (3)	1.72%	0.15	12.97%	2.62	152.43	6.75	3075.13	843.49	452.13	19.91
Goethite (3)	0.81%	0.19	12.04%	3.09	157.91	15.28	2195.07	469.90	468.59	17.58
Glassy Volcanic (8)	0.36%	0.32	7.50%	2.19	130.66	26.44	2227.53	283.76	481.11	61.39
Hematite (10)	0.57%	0.57	7.68%	1.71	134.94	21.60	2150.30	340.05	514.92	28.52
Weathered Fe (1)	3.49%		16.91%		173.97		2952.88		456.08	
BHVO-2 Standard	2.61%	0.03	13.81%	0.01	397.94	8.67	1708.51	6.71	176.36	0.48

Arthropod Presence Data

Data from 1,071 previously defined trapping locations, many of which were resampled each year, were compiled and sorted over 15 years spanning ~360 trapping days from 2001-2015, mainly from May-July (Brenner 2001-2006; Englund *et al.* 2007-2013; OMKM 2014-2015). Methods of trap preparations and construction are detailed in Office of Maunakea Management Standard Operation Procedure C (2015). A total of 690 trap locations were included within the TLS data extent and 1,030 locations (including all successful traps) were included within the 10 m DEM data extent (Figure 10). These samples were focused mainly on presence/absence in regions where wēkiu bugs have been found in the past and were not systematically placed or random stratified.

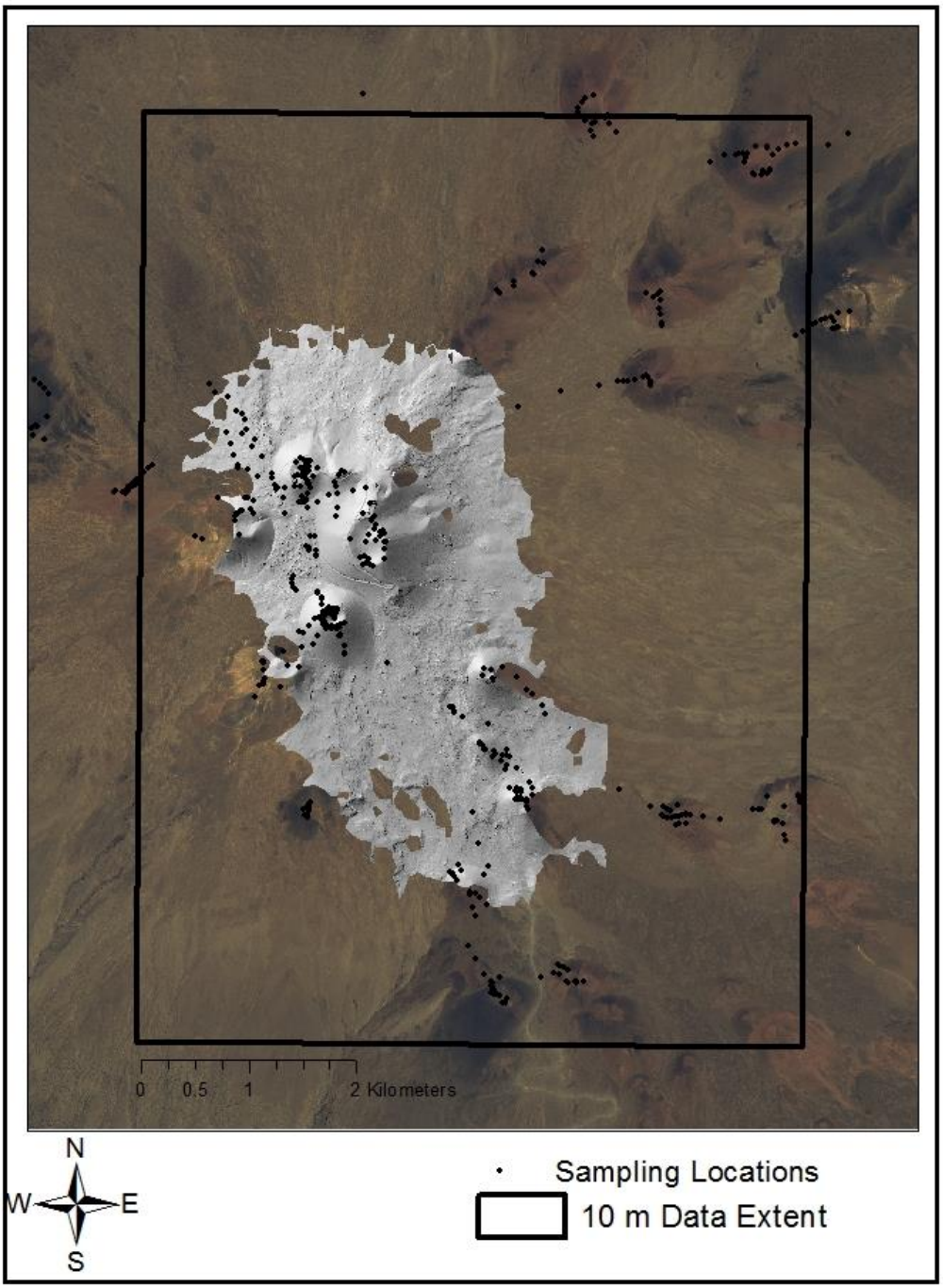

Figure 10: DEM derived from TLS data (shown as a hillshade image) contained 690/1071 total previous arthropod sampling locations (black dots). Available 10 m elevation dataset extent (black box) encompassed all sampling locations that were successful in trapping wēkiu bug(s).

Climate

Available annual average raster climate data including surface temperature, relative humidity, solar radiation, latent heat flux, rainfall, and actual evapotranspiration were obtained of the study area with a 250 m resolution (Giambelluca *et al.* 2013; Giambelluca *et al*. 2014). In order to run MaxEnt these datasets were resampled using bilinear interpolation from 205 m to 10 m and clipped to match the same pixel resolution and geographic extent as other data layers. We recognize that resampling continuous data to a finer spatial resolution is problematic, but without the availability of high resolution climate data we included available resampled data to test if any climate variables impacted model results. In order to test if climate heterogeneity or homogeneity existed among climate variables across the summit Principal Components Analysis (PCA) was performed. PCA analysis of climate variables (Figure 11) revealed that annual averaged climate has high homogeneity across the summit in 2014. Since climate data were only available at coarse spatial resolutions that needed to be resampled and because they showed high homogeneity, climate variables were not included in all models.

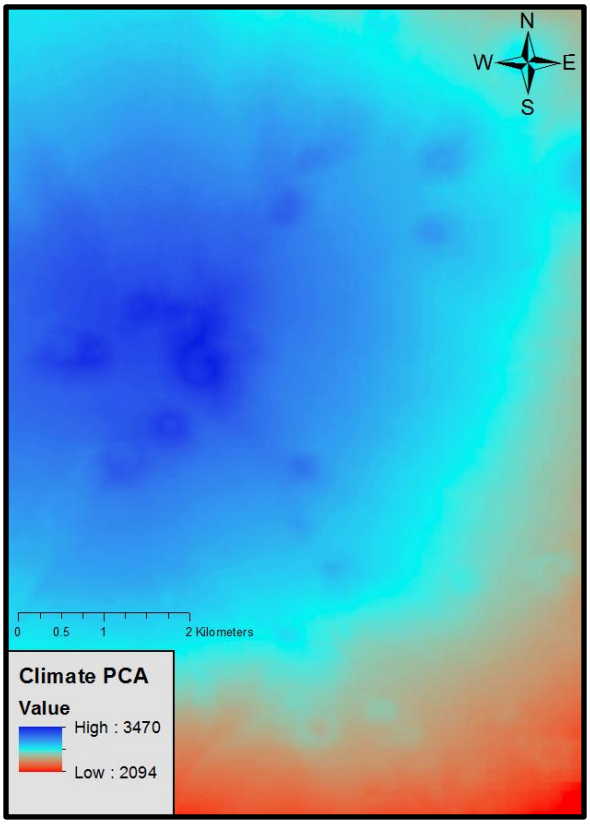

Figure 11: PCA of all climate variables included in MaxEnt Model C revealed that the summit has a high degree of climate homogeneity.

Maximum Entropy Habitat Suitability Modeling

MaxEnt v3.3.3k was used to run three habitat suitability models (Table 3) using the thresholds and settings detailed in Young *et al.* 2011.

Table 3: Three separate MaxEnt models run at different spatial resolutions with a combination of variables. Only Model C contained all habitat variables.

Name	Resolution	Slope, Aspect, Elevation	Mineralogy	Climate
Model A	1 m	X	X	
Model B	10 m	X	X	
Model C	10 m	X	X	X

Twenty percent of samples were withheld using a subsampling model evaluation method to test the overall model accuracy. Model A, run at 1 m spatial resolution, was limited to the extent of the TLS data (~15 km^2) while Models B & C (10 m) encompassed the entire study region (~55 km^2). Model outputs were maps with probability values ranging from 0 to 1, indicating the chance of encountering a species at any given pixel. Secondary outputs included tables which explained each variable's percent contribution to the model as a whole and permutation importance, which is a measure calculated by randomly permuting each variables values with species occurrence training data (Young *et al.* 2011). Jackknife analysis was enabled for all three models. Jackknife excludes each variable in turn and runs a model with all remaining variables, and also creates a model with each variable in isolation. This is an alternative measure of variable importance. The area under the receiver operating characteristic curve (AUC) statistic were calculated using a random percentage of species presence data and used to test models predictive power. An AUC statistic of 0.5 is equivalent to random while an AUC statistic of 1.0 means a perfect model fit (Phillips & Dudik, 2007; Elith *et al.* 2006).

RESULTS

Arthropod Presence and Terrain Characterization Results

Geoprocessing tools in ArcMap 10.3 were used to overlay arthropod presence (wēkiu bug trapping) data with appropriate cell values from derived habitat metrics including aspect, slope, elevation and depth to directly compare these variables with wēkiu bug captures. East and South facing aspects had higher average captures rates than North or West facing aspects (Figure 12A). Slope showed little variance between classes (Figure 12B), aside from >30 degree slope class, which had a statistically significant average capture rate with ~twenty-five bugs/day, but had a low overall sample size (19) and a single large capture (467 bugs) that dramatically inflated the mean. In terms of elevation, the 3700-3800 m and >4100 m elevation classes had significantly higher average capture rates than any of elevation classes (Figure 12C). Wēkiu bugs were not captured below 3500 m. Locations with depth information suggests that a depth of 0-5 cm is optimal, although a majority of samples were also taken at this depth (Figure 12D).

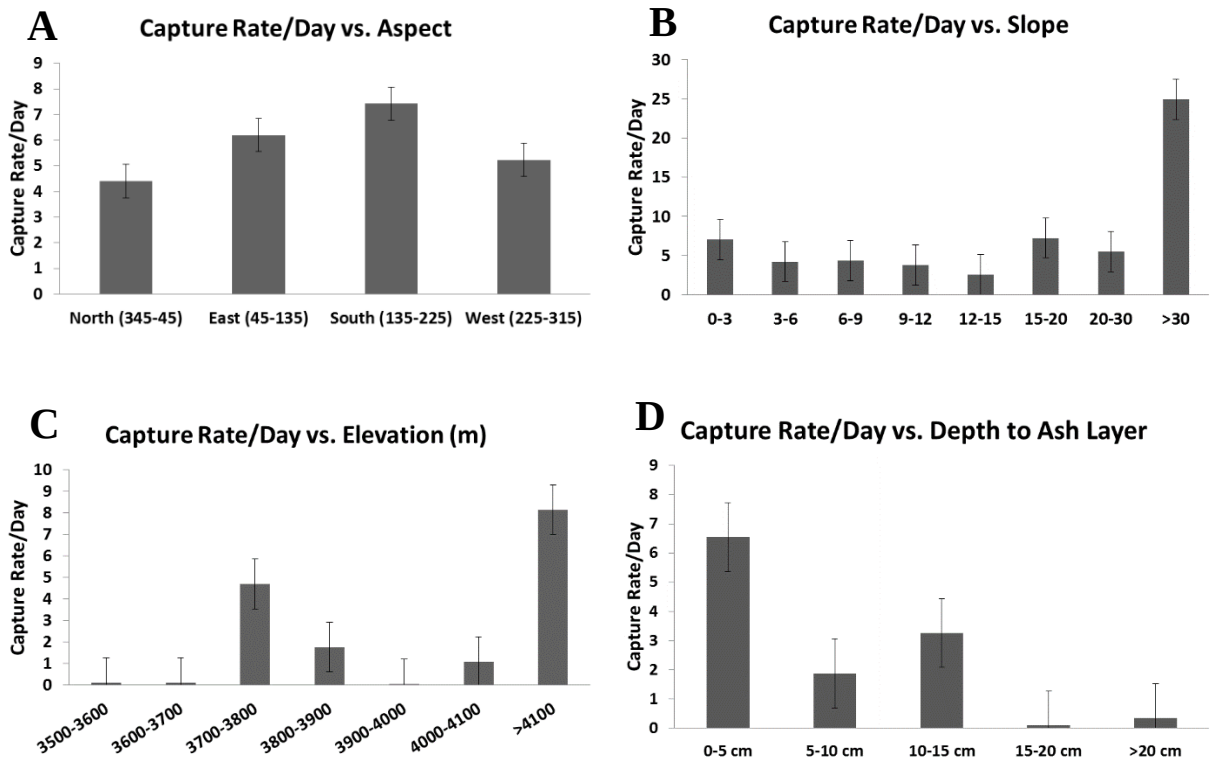

Figure 12: Wēkiu bug capture rates per day were directly compared for four terrain habitat variables (aspect, slope, elevation, depth to the underlying ash layer).

Mineral Characterization Results

Geoprocessing tools in ArcMap 10.3 were used to overlay arthropod presence data with the 0.5 m surface mineralogy classification (Figure 6) and extract appropriate cell values. Comparing surface mineralogy with fifteen years of trapping data reveals disparities in wēkiu bug trap success and average capture rates with mineralogy (Figure 13). Of the 6 mineral types present, only five had recorded captures and only hematite and glassy volcanic rock produced captures in >40% of the traps. Hematite displayed the highest average capture rate and overall success rate. Both amorphous Fe- hydroxides and Fe 2+ minerals had low average capture rates but modest success rates. Weathered Fe mineral class had a single successful capture in 32 samples and Goethite had zero successful captures. A binomial logistic model yielded significant statistical differences between presence/absence of wēkiu bugs in hematite, glassy volcanic rock, and amorphous Fe- hydroxides, and no statistical differences between the remaining minerals (Table 4).

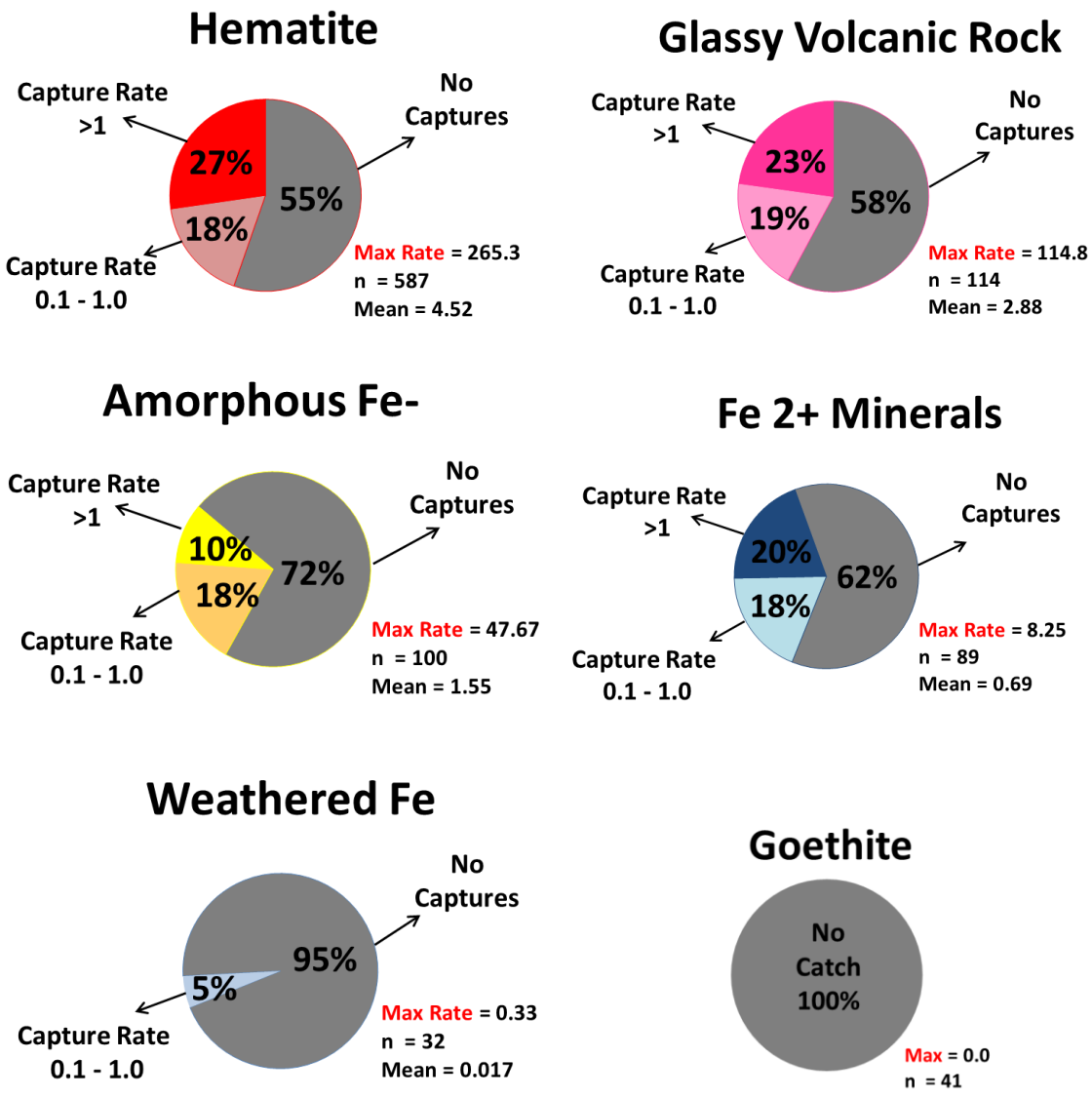

Figure 13: Wēkiu bug trapping locations were overlaid with surface mineralogy classification and mineral values extracted using geoprocessing tools so that mineralogy could be directly compared to wēkiu bug capture rates. Samples were not evenly distributed amongst mineral classes.

Table 4: Binomial logistic model results indicating that hematite, glassy volcanic rock and amorphous Fe-hydroxides were statistically significant (p-value <0.05) in terms of the presence of wēkiu bugs.

*Goethite's extreme standard error is a function of a small sample size and no successful captures.

Degrees of Freedom	963			
Mineral	Sample Size	Estimate	Std. Error	P-Value
Hematite	587	0.73	0.23	<0.005
Glassy Volcanic	114	0.63	0.29	<0.05
Goethite*	41	-15.62	374.75	0.97
Fe 2+ Minerals	89	0.53	0.31	0.09
Weathered Fe	32	-1.95	1.05	0.06
Amorphous Fe-	100	-0.94	0.22	<0.005

2015 Mineralogy and Geomorphic Position Arthropod Survey

Since hematite had the highest maximum capture rate, average capture rate, and a success rate >40%, we hypothesized that hematite surface minerals on cinder cones represented a higher degree of suitable habitat than other surface minerals on or off cinder cones above an elevation threshold. Geomorphic position (cinder cone vs. toe, defined as an obvious slope/elevation break) may also play an important role in wēkiu bug spatial patterns, dictating microclimate and aeolian food availability, and may give insight into habitat use and other community dynamics on a per cinder cone basis. To test these hypothesis regarding surface mineralogy and geomorphic position, we carried out a stratified random sampling experiment along a cinder cone in an area that had not been previously sampled. Sixty-two total live-baited pitfall traps were placed on the backside of Puʻuwēkiu in October, 2015, adhering to Office of Maunakea Management Standard Operation Procedure C (2015) (Figure 14). Twenty traps were placed on a sloping portion of the cinder cone with predominantly hematite surface minerals. Another twenty traps were place on the cinder cone toe with a lesser degree of slope ranging from 5.0-11.0 degrees, but still predominantly hematite. An additional twenty traps were placed below the cinder cone toe in various other minerals aside from hematite. Two traps were placed on a sloping portion in glassy volcanic rock adjacent to hematite. Trimble XH 6000 GPS units were used to occupy geographic positions for five minutes at each trap site and differentially corrected in GPS Pathfinder Office. A majority of the recorded point locations had a positional accuracy between 5-15 cm. Depth to the underlying ash layer was recorded (in cm) at each location. Live-baited pitfall traps were re-visited and collected after 3 days and the number of wēkiu bugs recorded. Other arthropod contents were sorted, counted, and released (live caterpillars were

collected and reared in captivity for adult moth emergence and species identification, confirmed as a known *Agrotis* new species yet to be described, family Noctuidae) (Eiben, Personal Communication, 2015).

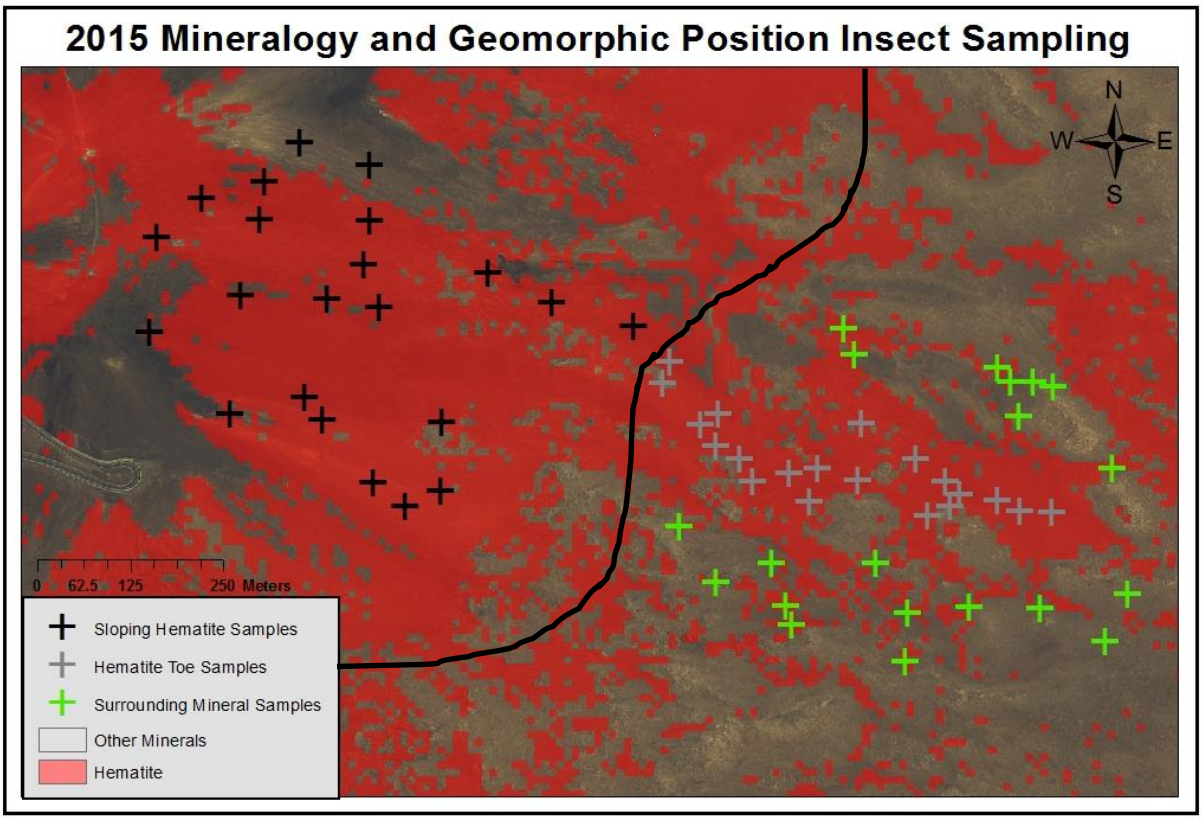

Figure 14: 2015 experimental design showing different sets of live arthropod traps testing different habitat variables. Black +'s represent traps placed in hematite on the upper sloping portion of a cinder cone while the grey +'s represent traps placed in hematite on the cinder cone toe with a relatively flat slope. Green +'s are traps placed in surrounding minerals other than hematite with a flat slope. The black line represents the border between the primary cinder cone slope and the cinder cone toe derived using elevation and slope breaks.

This stratified random mineralogy and geomorphic position experiment successfully trapped wēkiu bugs in an area that had not been previously sampled. A total of 49 wēkiu bugs from 20 live arthropod traps were captured directly on a steep sloping portion of a cinder cone section consisting of predominantly hematite, for an average of 2.45 bugs/trap (Figure 15). These higher elevation hematite traps had a success rate of 60% (12/20) but patterns of species presence and absence were most likely driven by predation, with a number of known predatory species individuals captured in the area. Two wēkiu bugs were caught in a steep sloping portion of glassy volcanic rock directly adjacent to a large expanse of hematite. No wēkiu bugs were

caught below the cinder cone toe in either hematite or other minerals (see discussion). Various other arthropods were also captured including wolf spiders (Lycosidae, *Hogna* sp.), sheet web spiders (Linyphiidae), *Agrotis* caterpillars (Noctuidae, *Agrotic* n. sp.), seed bugs (Lygaeidae, *Nysius palor),* and unknown species and families of mites, aphids (Aphididae), springtails (Entomobryidae) and flies (mostly Sciaridae)(Eiben, Personal Communication, 2016). Previous arthropod trapping data came from summer months (May-July) while this experiment was conducted in the fall and may reflect seasonal community dynamics.

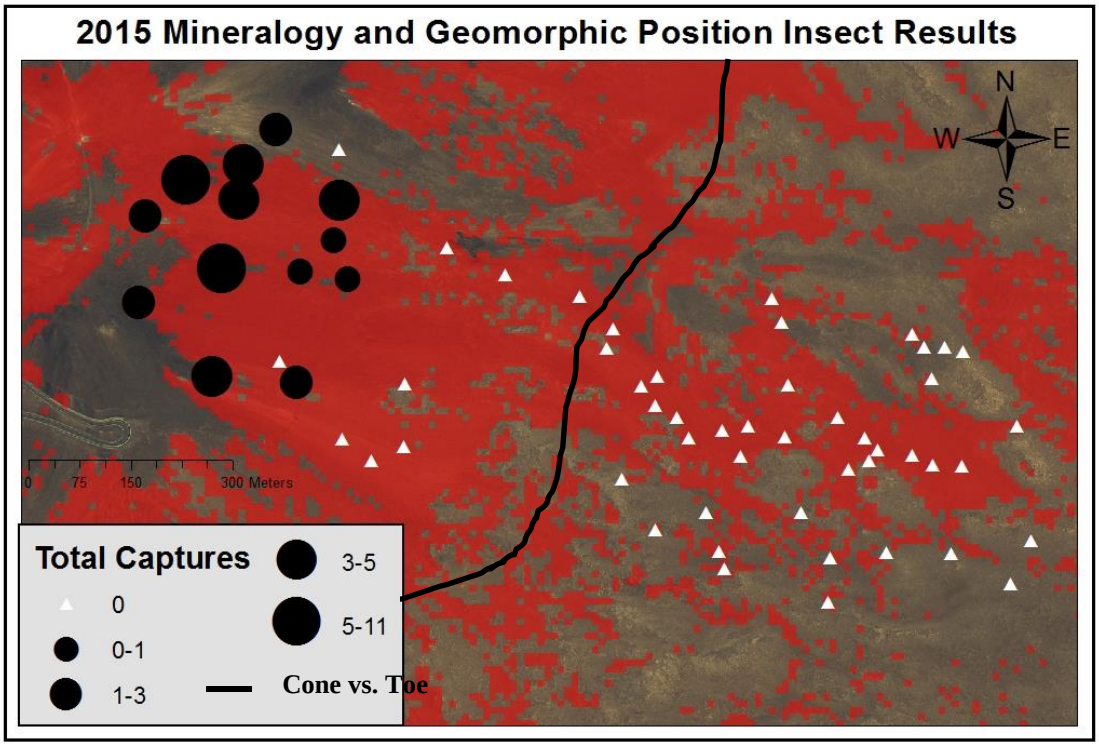

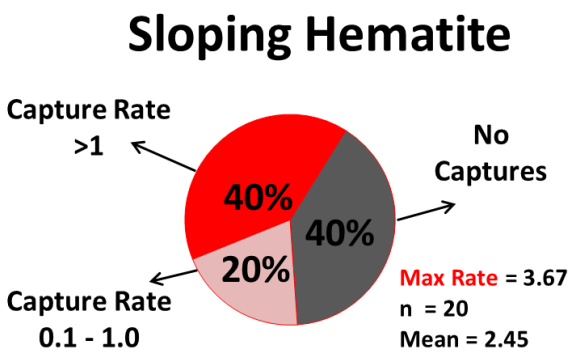

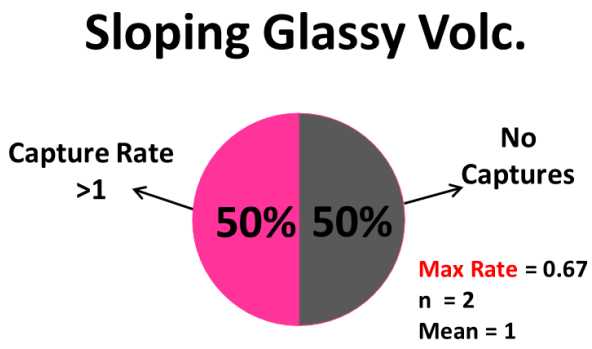

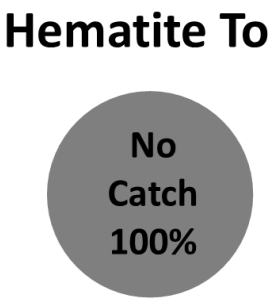

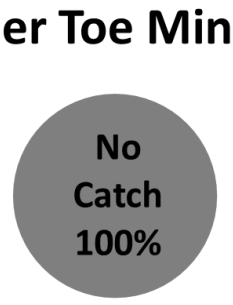

Figure 15: 2015 insect survey results show that wēkiu bugs were only captured on a sloping portion of a cinder cone in hematite (graduated black dots) and no wēkiu bugs were caught elsewhere (white triangles) aside from two wēkiu bugs caught in glassy volcanic rock. Pie charts show trap success rates, maximum and average capture rates.

Maximum Entropy Habitat Suitability Modeling

MaxEnt was used to generate predictive habitat suitability models at two different spatial resolutions and extents. The first model, Model A, was limited to the ~15 km^2 of 1 m TLS data and incorporated 366 presence locations along with mineralogy, elevation, slope and aspect. Model A shows that the summit cinder cone complex (Puʻuhaukea, Puʻuwēkiu, Puʻukea, Puʻuhauʻoki) harbors the greatest area of suitable wēkiu bug habitat in this area (Figure 16). Portions of cinder cones including Puʻupoliʻahu, Puʻulilinoe and VLBA North and South also have sections highlighted as suitable. The habitat variables with the largest percent contributions to Model A were elevation (62.2%), hematite (17.6%), and aspect (8.4%), with minor contributions from other variables (Table 5). Jackknife analysis reveals that elevation, hematite, and aspect, account for the largest contributions to the model when run in isolation (Figure 17). The average AUC statistic using a subsampling validation technique was 0.856 (StDEV=0.029) for test data, signifying these habitat variables were significantly better than random. Although this model does not cover the entire known geographic range of wēkiu bugs it does encompass the historic population center and many of the locations where wēkiu bugs have been trapped in the past.

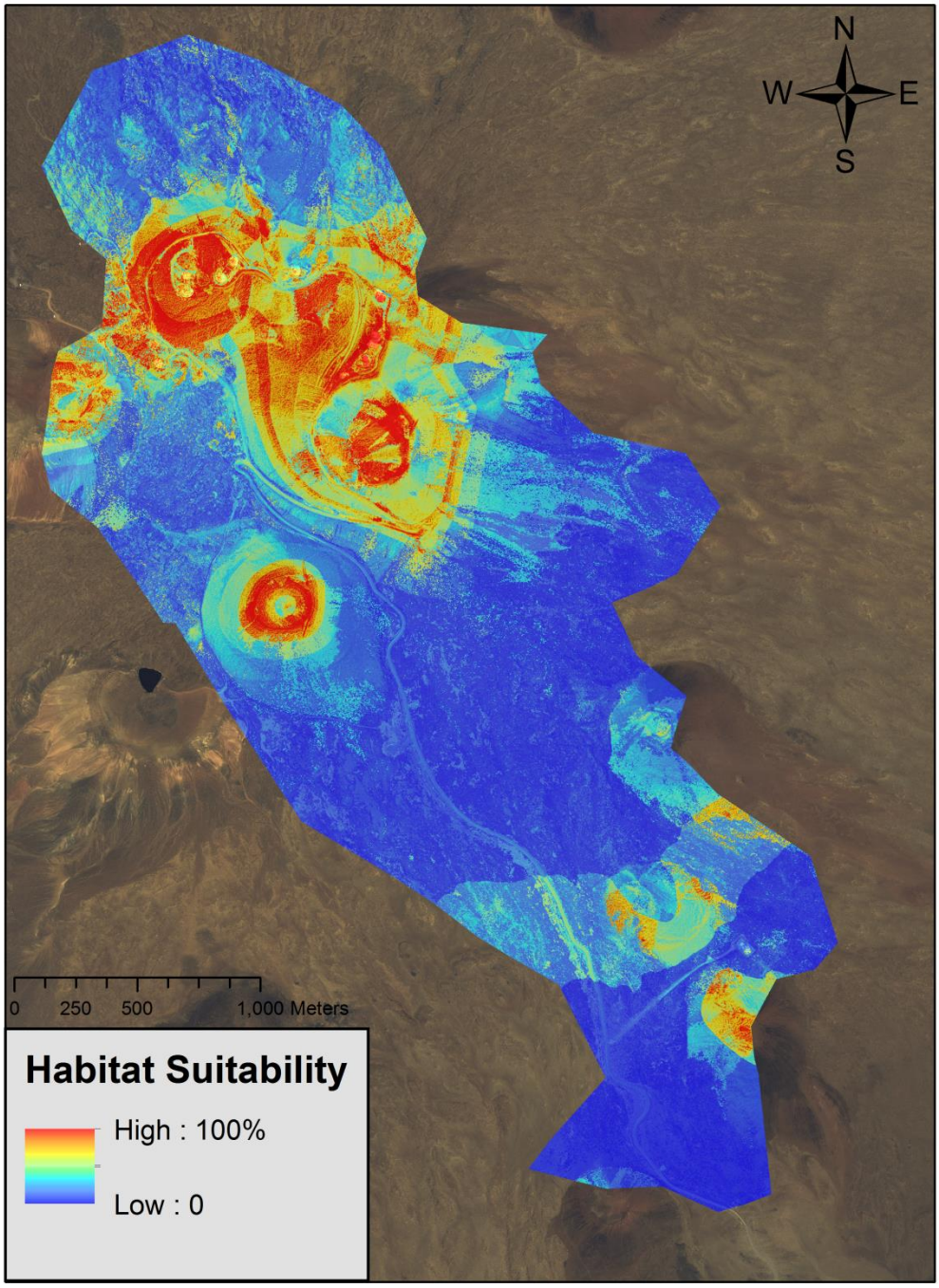

Figure 16: Model A (1 m) generated from species occurrence data, elevation, slope, aspect and surface mineralogy highlights areas of increased habitat suitability for wēkiu bugs.

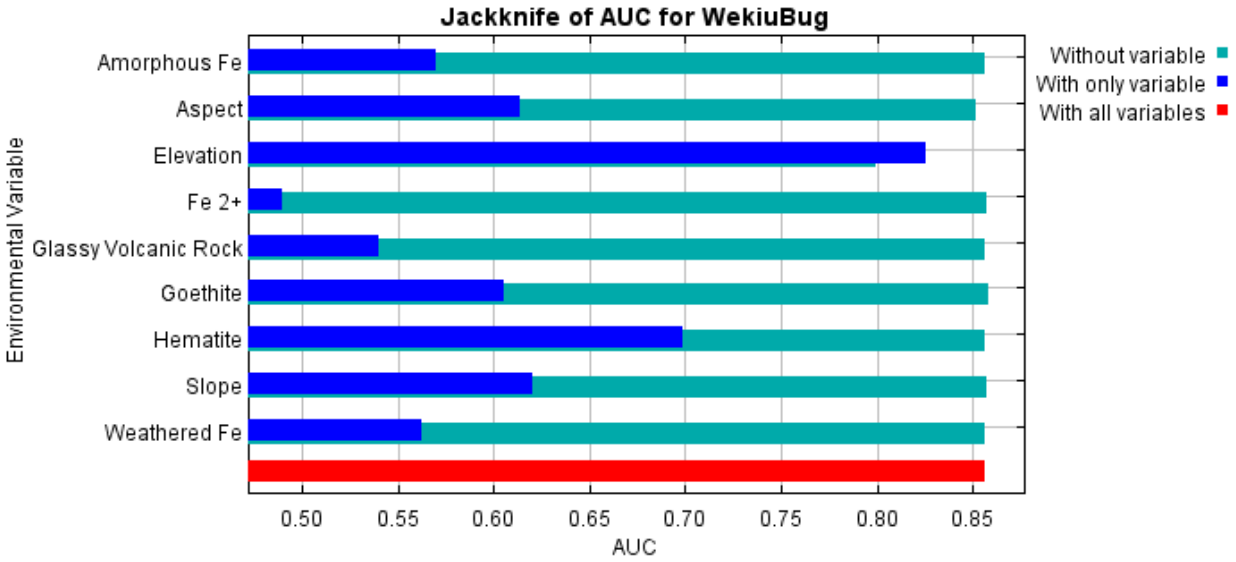

Figure 17: AUC for Model A. Elevation, when ran in isolation, accounted for the largest proportion of the model followed by hematite and aspect.

The additional models, Models B and C, both included the same habitat variables as Model A but at a 10 m spatial resolution over a larger study region (Figure 18). In addition, Model C also included resampled climate data, which was not used in either Models A or B. Similar to the finer resolution Model A, Models B and C both highlight the summit cinder cone complex as suitable. These expanded models also include sections of other cinder cones such as Pu‘upoli‘ahu, Pu‘ulilinoe, Pu‘umāhoe, Pu‘upoepoe, and Pu‘uala and small portions of Pu‘umākanaka as suitable habitat (see Figure 2 for place names). Model B (excluding climate) shows that elevation and hematite have the highest model contributions at 78.2% and 13.7%, respectively. Jackknife analysis affirms this as well (Figure 19). Average AUC values were 0.947 (StDEV=0.009) for test data. Model C (including climate) differed in that the highest model contribution was attributed to elevation 36.5% and relative humidity 25.6%, while the highest permutation importance was elevation 82.7, and actual evapotranspiration 10.7 (Table 5). Jackknife analysis reveals that elevation, evapotranspiration, relative humidity and surface temperature, each account for a large portion of the model when run in isolation (Figure 20) likely because of auto-correlation among climate variables. The average AUC values were 0.965 (StDEV=0.008). Considering Model B encompassed all successful wēkiu bug trapping locations, had an acceptable AUC statistic, and the fact that climate data were excluded from the final

analysis (see discussion), it was used to define suitable wēkiu bug habitat (in terms of percent contribution) as high elevation (78.2%) and the presence of altered nanocrystalline hematite surface minerals (13.7%), on select portions of summit cinder cones.

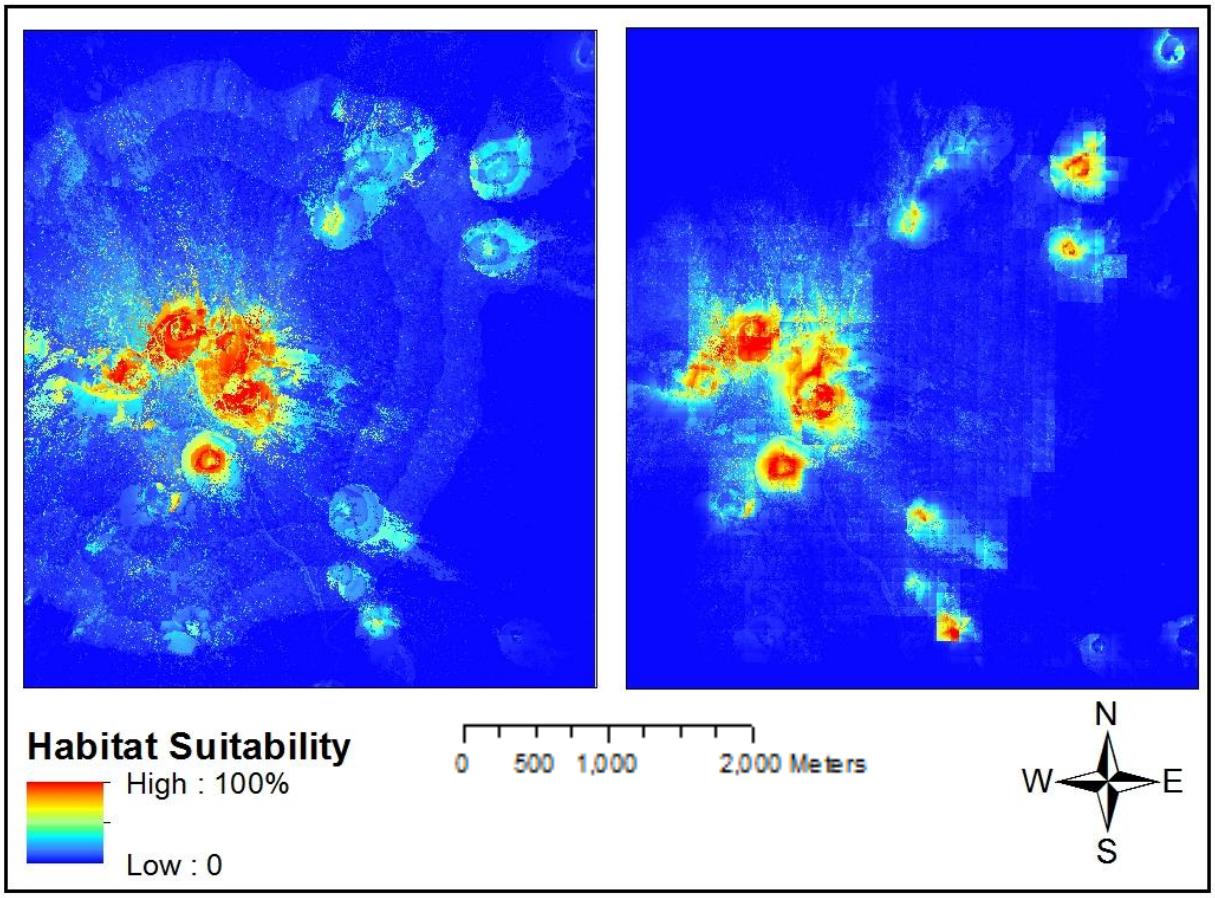

Figure 18: Model B (left) excluded climate variables and Model C (right) included climate variables. Both models generally agree where areas of suitable habitat and marginal habitat for wēkiu bugs are located.

Table 5: Environmental variable importance analysis measured by percent contribution and permutation importance of MaxEnt Models A, B, and C.
*Models B and C covered the same area while Model A covered a subset of that area.

Environmental Variable	Percent Contribution			Permutation Importance		
	Model A	Model B*	Model C*	Model A	Model B*	Model C*
Elevation	62.2	78.2	36.5	53.5	89.1	82.7
Aspect	8.4	0.4	1.2	11.9	0.2	0.5
Slope	2.8	0.6	1.2	5.1	0.6	0.1
Hematite	17.6	13.7	10.5	13.1	1.9	0.3
Amorphous Fe	1.8	2.7	1.9	3.8	1.8	0.2
Weathered Fe	2.4	2.1	1.6	1.8	4.3	0.6
Goethite	3.3	1.6	1.4	3.8	0.6	0.3
Glassy Volcanic Rock	0.7	0.7	0.2	4.0	0.6	0.0
Fe 2+ Minerals	0.8	0.0	0.0	3.0	0.0	0.0
Relative Humidity	-	-	25.6	-	-	0.3
Solar Radiation	-	-	13.7	-	-	1.3
Evapotranspiration	-	-	2.6	-	-	10.7
Rainfall	-	-	2.1	-	-	1.6
Latent Heat	-	-	1.0	-	-	0.9
Surface Temperature	-	-	1.4	-	-	0.4

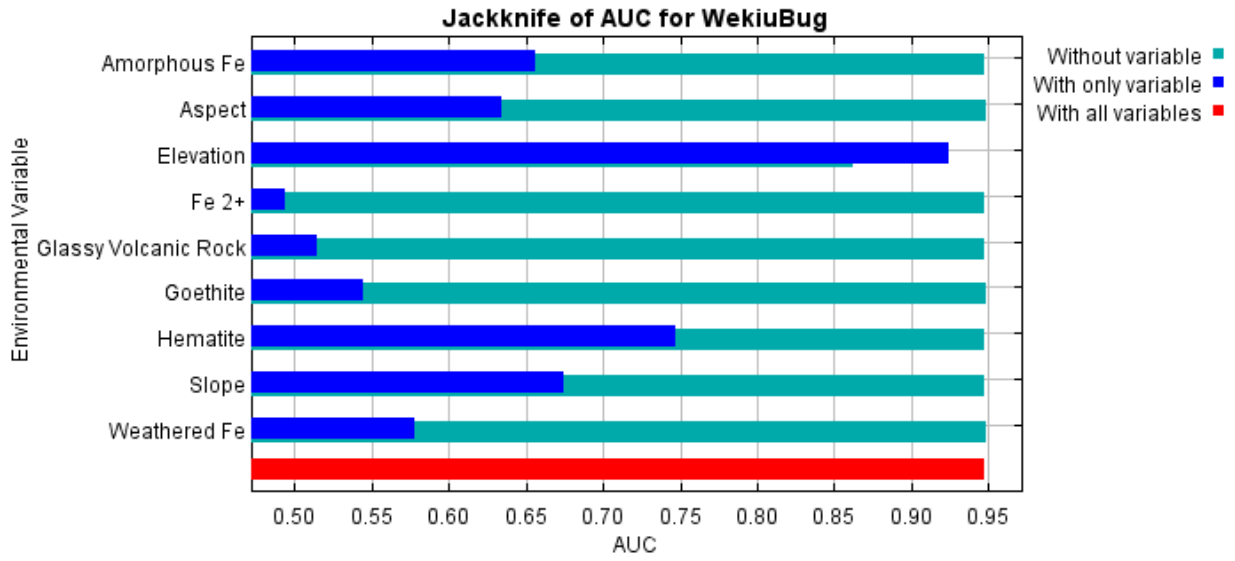

Figure 19: AUC for Model B shows that elevation, when run in isolation, accounts for the largest proportion of the model followed by hematite.

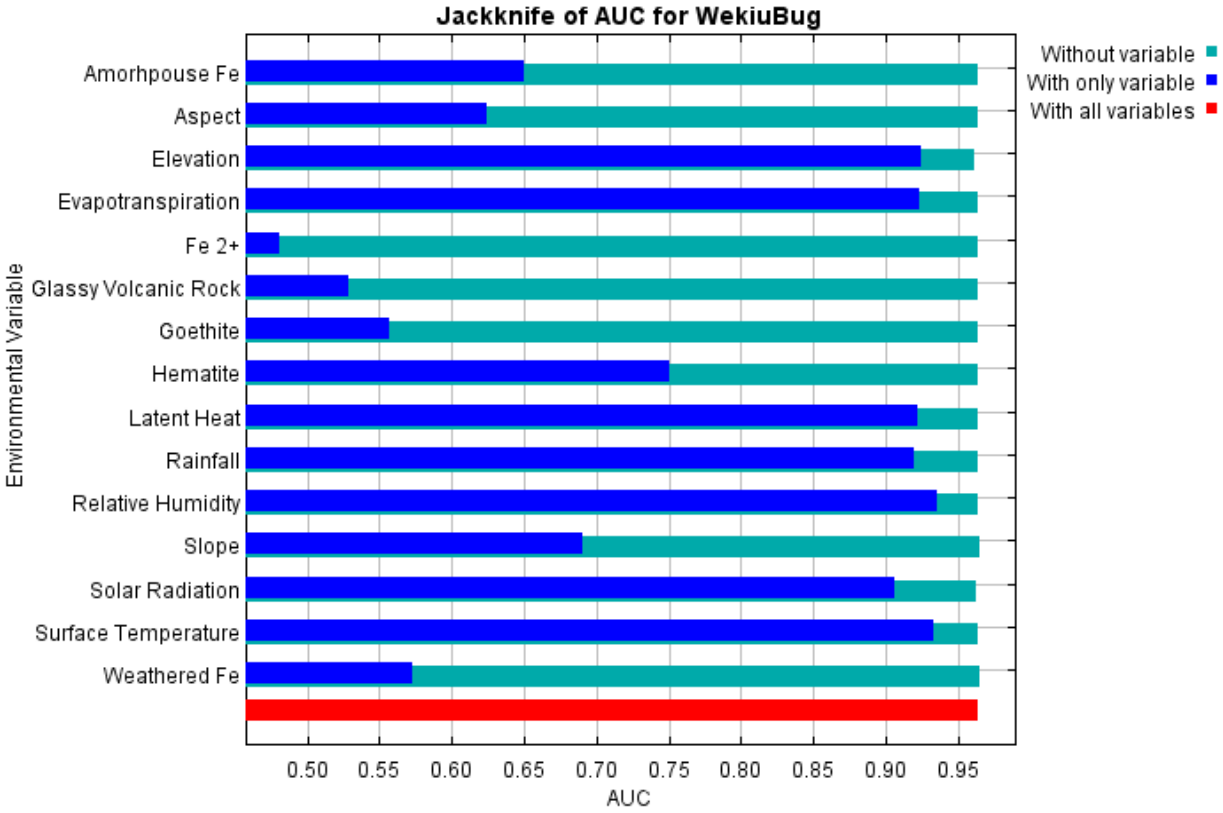

Figure 20: AUC for Model C show that a number of variables, when run in isolation, account for large portions of the model, most likely due to high collinearity between climate variables.

DISCUSSION

Topographic Terrain Characterization

We successfully demonstrated that lidar occlusions can be accurately patched with imagery collected from terrestrial and airborne camera campaigns. Lessons learned include the importance of creating enough overlap between the raw lidar and SfM point clouds to be able to register them together in CloudCompare, instead of solely relying on differential GPS coordinates for ephemeral ground control points. Successfully patching two lidar occlusions allowed us to calculate values for habitat metrics at nearly all wēkiu bug trapping locations that would otherwise have been interpolated from much coarser resolution datasets.

Comparing the last fifteen years of wēkiu bug trapping data to topographic variables, trends were found for both elevation and aspect. These trends only reflect habitat utilization during summer months (May-July) given available trapping data and may change seasonally. Elevation classes 3700-3800 m and >4100 m had significantly higher captures than all other elevation classes. This is likely a function of the elevation bands at which different cinder cones are found (for example Puʻukea, Puʻuwēkiu and Puʻuhauʻoki have all the same relative elevations). East and south facing slopes produced higher average capture rates (6.2 & 7.4 bugs/day) than north or west facing slopes (4.4 & 5.2 bugs/day) (Figure 12A). Samples were not evenly distributed among aspect classes (North n=107, East n=165, South n=145, West n=215) but even so, we believe these results are indicative of wēkiu bug summer geographic distributions and would not change with equal sampling. South facing cinder cone slopes were associated with the highest average captures rates, while north facing slopes had the lowest average capture rates. This may be a function of solar radiation intensity and duration, with south facing slopes receiving more intense and longer duration solar radiation than north facing slopes which are shaded by local topography. Wēkiu bugs have been observed basking on rocks and possibly use this intense solar radiation to thermoregulate. Higher average temperatures on south facing slopes would also allow faster and more total energy accumulation for accelerated wēkiu bug growth and reproduction given Degree Day Modeling of insect growth rates (Eiben & Rubinoff, 2014).

Depth measurements were collected at 71 locations with associated wēkiu bug traps and revealed that an optimal depth lay between 0-5 cm from the topmost rock layer down to the ash layer, although the vast majority of depth samples (51) were at this depth and may not be indicative of the true optimal depth layer needed for thermoregulation and protection from predators (Eiben & Rubinoff, 2014). In order to accurately assess if any relationships exist between depth to the underlying ash layer and the number of wēkiu bugs captured more samples are needed, in addition to a greater understanding of depth to the ash layer spatially across the summit. It is likely that increased wēkiu bug captures are associated with a depth threshold, beyond which would be ideal, and below which would be marginal.

Comparing fifteen years of summer trapping data with slope classes did not yield any significant trends, although the >30 degree slope class had a much higher average capture rate than all other slope classes. This can be attributed to a single large capture (467 wēkiu bugs) and low overall sample size (19) within this class. If this single large capture were removed the average capture rate per day for >30 degree slope class would be more similar to other slope classes. The fact that wēkiu bugs were successfully captured in all aspects but no trends were found for slope suggests that wēkiu bugs utilize entire cinder cones from toe to rim during the summer, as opposed to persisting on any given aspect or slope alone during the summer months. Summer may be when wēkiu bug populations are greatest and they inhabit the maximum extent of their suitable habitat range, potentially even expanding to the fringes and into marginal suitable habitat.

Wēkiu bug distributions may vary within their specific habitat range throughout the year. The results discussed so far were generated from summer presence activity only and do not take into consideration potential population movements throughout the season. Climate variables such as wind speed and predominant direction, as well as sun track changes throughout the year (Giambelluca *et al.* 2014; Silva & Businger, 2006) may affect the intra-annual or seasonal variability in wēkiu bug geographic distributions by affecting the availability of aeolian deposited insect prey and potentially altering the way rock tephra heats and cools. Additional wēkiu bug trapping is planned for 2016-17 taking into account aspect, slope and surface mineralogy, as well as measuring surface, sub-surface and ash layer temperatures and relative

humidity every three months and should sufficiently capture any large population movements (if they exist) and help to explain habitat dynamics and cinder cone use seasonally.

Mineral Characterization

The AVIRIS-derived 0.5 m spatial resolution surface mineralogy classification reveals disparities in the average capture rate of wēkiu bugs and trap success rates with mineralogy. Traps were considered successful if one or more wēkiu bugs were captured. Traps located in hematite and glassy volcanic surface minerals displayed the highest average capture and trap success rates, compared to any other mineral classes. Summit cinder cones are predominantly composed of Hawaiite basaltic lava which was altered during or after emplacement into hematite and glassy volcanic rock surface minerals, aside from hydrothermally altered Pu‘upoli‘ahu and Pu‘uwaiau which are largely composed of Fe 2+, amorphous Fe- hydroxides, hematite and small amounts of goethite (Swayze *et al*. 2002). Observationally, hematite rocks contained various sized vesicles and were naturally sorted in a way that contained numerous interstitial spaces, and on average had less places with ash at the surface when compared to other mineral types. It has been hypothesized that wēkiu bugs require these interstitial spaces to be able move up and down the cinder column for thermoregulation and may use vesicles to hide from larger predators (Eiben & Rubinoff, 2014, 1086). Hematite and glassy volcanic rock have also been sampled in much more than other mineral types because of their association with most cinder cones on the summit. In the past cinder cones were identified as prime wēkiu bug habitat resulting in the vast majority of traps being placed on or near cinder cones because presence and occupied range data were required at that time. Arthropod traps placed in glacial till/lava flows and along roadways were mostly meant to monitor for potentially invasive species such as ants or wasps and collect species richness and abundance data for arthropods other than wēkiu bugs. Even so, given the high success rates for traps placed in surface minerals associated with most summit cinder cones, and low success rates in surface minerals outside of cinder cones, we believe these general trends would remain given equal sampling.

2015 Mineralogy and Geomorphic Position Arthropod Survey

The 2015 Mineralogy and Geomorphic Position Arthropod Survey (Figure 14) affirmed that surface mineralogy and geomorphic position both play a significant role in the spatial

patterns of wēkiu bugs (Figure 15). The high presence of wēkiu bugs near the hematite cinder cone rim and absence downslope on the flatter portion of the cinder cone toe/tail suggests that sloping portions of cinder cones with predominately hematite surface minerals represent a higher degree of suitable habitat, although multiple habitat variables, which have yet to be assessed, may also be at play (such as substrate compression in cinder cone craters). Local scale climate variables such as surface temperature or relative humidity may play a significant role in creating microhabitats and/or uninhabitable regions but could not be evaluated with available 250 m data. Geomorphic position along a cinder cone may also be related to food and water availability. For example, cinder cones facing predominant wind patterns may receive higher concentrations of aeolian deposited insect prey than on other sides of the same cinder cone or cinder cone toe.

Competitive exclusion and predation may also affect wēkiu bug distributions. Wēkiu bugs seemingly do not have natural defenses, other than avoidance, against predators such as spiders or caterpillars. A large number of *Agrotis* caterpillars were captured mid- and down-slope of the cinder cone rim (Figure 21) which may explain the absence of wēkiu bugs in the traps at those lower elevations. *Agrotis* caterpillars are natural predators as omnivores in the alpine environment (Duman & Montgomery, 1991) and both *Agrotis* and wēkiu bugs were only captured simultaneously in 2 out of 62 traps. *Agrotis* caterpillars may have consumed wēkiu bugs in their entirety prior to trap collection.

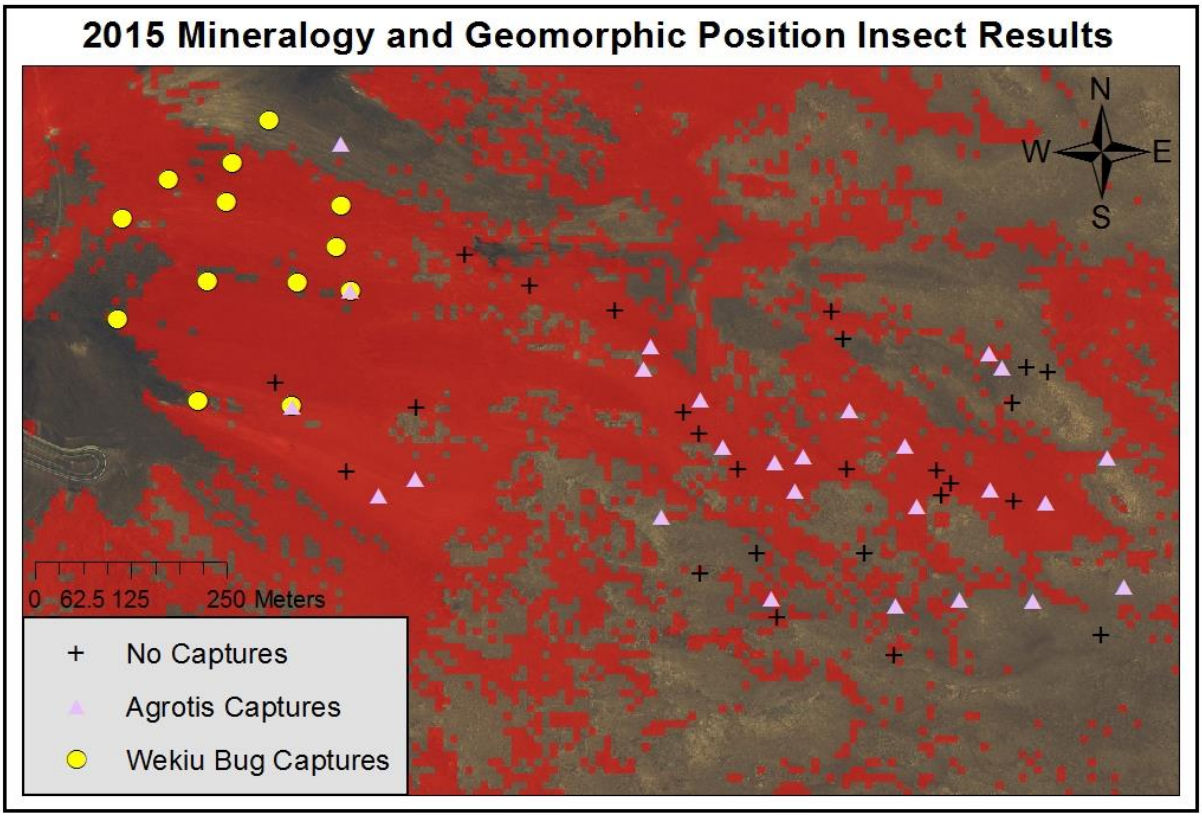

Figure 21: 2015 experimental trap results shows the locations of wēkiu bug and *Agrotis* caterpillar captures on the eastern side of Pu‘uwekiu. Yellow dots represent successful wēkiu bug captures, purple triangles represent successful *Agrotis* captures while black +’s represent the absence of wēkiu bugs and *Agrotis*, but presence of other species, or no captures entirely.

Unlike the rest of the arthropod survey data in this thesis, the 2015 experimental arthropod survey was conducted in the fall (October). This temporal difference may give potential insights into habitat use and population activity seasonally. Wēkiu bug populations may be at their lowest activity rates during winter months and may retreat to core areas of suitable habitat to maximize survival. This may be unlike summer months where wēkiu bugs may be more active, expanding their spatial extent and population size. This could mean that the upper portions of cinder cones and cinder cone rims represent a higher degree of suitable habitat than lower portions of the same cinder cone throughout the year. This is further supported by the fact that the majority of large captures are on upper portions of cinder cones. The movement from higher elevations to lower elevations on the same cinder cone could be a seasonal cycle which could potentially be captured during multiple sampling events throughout the year.

Maximum Entropy Habitat Suitability Modeling

MaxEnt model A (Figure 18) shows that elevation and mineralogy play significant roles in wēkiu bug capture rates and locations, although as stated earlier, sampling efforts were not evenly distributed over space or amongst mineral classes with relatively low number of samples in weathered Fe (32) and goethite (41). Model A shows that locations with the highest probability of encountering a wēkiu bug are on or near cinder cone rims, including lower portions of cinder cones but excluding lava flows and other areas outside of cinder cone boundaries, suggesting that wēkiu bugs are almost entirely restricted to cinder cones. This also suggests that, although the known wēkiu bug geographic range is above 3350 m, wēkiu bugs display habitat specificity, which means that overall wēkiu bug range may be relatively large but the actual area of suitable and occupied habitat are much smaller. At a micro-level, this 1 m resolution model can identify small regions of suitable microhabitat that coarser resolution models may miss or lump together (Figure 22). That said, the different resolution models largely agree on the locations of suitable and unsuitable habitat and therefore high resolution data may not add enough information to warrant the added expense and time needed to acquire and process.

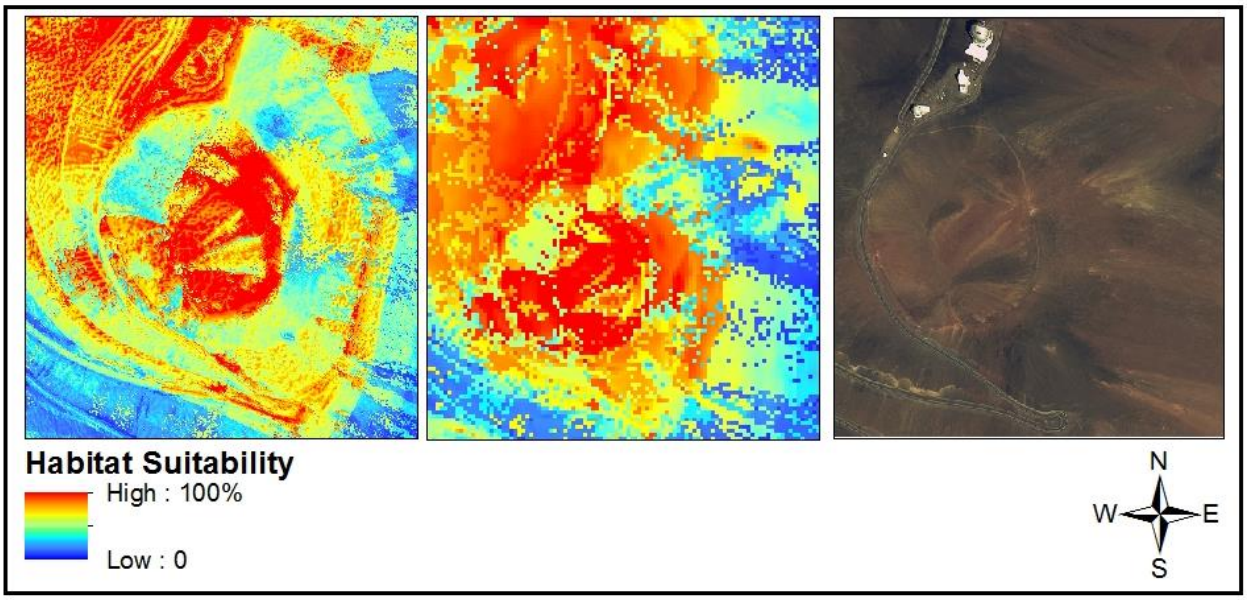

Figure 22: Side-by-side comparison of Model A (1 m), Model B (10 m), generated using MaxEnt with the same ecogeographical habitat variables and species occurrence data, and 0.5 m WorldView 2 satellite imagery for reference. The higher resolution Model A identifies small regions of unsuitable habitat that Model B identifies as suitable of the summit cinder cone Pu‘uwēkiu’s crater.

MaxEnt Model B, which excludes climate, and Model C, which includes climate (Figure 20) generally agree on the locations of suitable habitat, suggesting that climate plays a minimal role in the spatial patterns of the wēkiu bug (at least at 250 m resolution). Model C does show increased habitat suitability in certain locations that Model B displays as marginal habitat, such as VLBA south, Puʻupoepoe, and Puʻuala, which is worth exploring during future sampling efforts. Certain climate variables also showed high collinearity which can mask the importance of a climate variables contribution to the model, create higher model variance (Meloun *et al.* 2002), and undoubtedly add to model complexity and uncertainty (Braunisch *et al.* 2013). PCA of climate variables revealed that the summit has a high amount of climate homogeneity and thereby reaffirms, at this resolution, that climate is not dictating the spatial patterns of successful wēkiu bug captures. Wēkiu bugs can only grow and reproduce in temperatures between 11-32^{o}C (Eiben & Rubinoff, 2014) which means climate variables such as solar radiation and surface temperature are undoubtedly important but are not informative at the current spatial resolution. Climate data were excluded from the final analysis and definition of suitable wēkiu bug habitat because of these reasons: auto-correlation, scaling limitations and the lack of sufficient weather stations near the study area, highlighting the need for higher resolution climate data for a more robust analysis (Franklin *et al.* 2012). The percent importance of low relative humidity (25.6%) in Model C may be indicative of the interplay between substrate type and climate and can be assessed in greater detail when higher resolution climate data becomes available. If higher-resolution climate data becomes available we can also model suitable range contraction or expansion given projected climate change data, which may help guide future management strategies (Loarie *et al.* 2008; Wiens *et al.* 2009; Rochlin *et al.* 2013). In order to test the validity of produced wēkiu bug suitability habitat models, independent and/or new species data spanning the range of possible environmental space must be collected. This will serve to evaluate the predictive power and reliability of the habitat suitability models (Vaughan & Ormerod, 2003). Each annual arthropod trapping season led by the Office of Maunakea Management can serve as an iterative process that evaluates and refines future suitability models.

Trapping locations were not originally arranged with a habitat suitability model in mind but focused on previously successful areas along an elevation gradient, to assess population structure and relative density estimates, and to detect any potential invasions from predatory

arthropods. Many of these traps were placed near roads and other accessible pre-determined locations instead of being systematically or randomly placed across the summit. This means that our results are likely biased and may not be fully indicative of true species distribution (Syfert *et a*l. 2013; Kadmon, R. *et al*. 2004; Kramer-Schadt et al. 2013; Phillips *et a*l. 2009), although Costa *et al*. (2009) has shown that even with geographically biased sampling locations, model results can be robust and predictive of species distributions in regions previously not sampled. These models can be used to identify potentially suitable regions that have been historically under sampled, such as some of the remote cinder cones, which only have a few total samples, or portions of cinder cones that are routinely sampled but other have portions of the same cinder cone that are not well represented.

Wēkiu bugs displayed a high amount of habitat specificity, being restricted only to summit cinder cones. This describes one classic definition of a rare species: narrow geographic range (Maunakea summit >3350 m) and narrow habitat specificity (summit cinder cones) (Rabinowitz, 1981, 2010; Isik, 2011). This means that total species geographic range and actual occupied range are not equivalent, with occupied range being a considerably smaller area. These findings are broadly similar with other narrow restricted range endemic species that have adapted to specific habitat conditions and persist in subsets of their total geographic range (Ribeiro & Fernandes, 2000; Kruckeberg & Rabinowitz, 1985). Habitat suitability models for species that have narrow ecological ranges have been shown to have higher predictive accuracy than for species that have widespread geographic distributions and low habitat specificity (Segurado, P. & Araujo, M. 2004; Franklin *et al.* 2009). Species with limited geographic ranges appear to have higher densities of individuals near the center of their range slowly declining towards range edges and into marginal habitat (Brown, 1984). This may explain why the majority of high captures and consistently high trapping locales are concentrated in the summit cinder cone complex which also represents the largest area of suitable habitat.

Suitability Modeling of Other Summit Species

Compiling the necessary data to model wēkiu bug suitability now allows us to model many other arthropod species on the Maunakea summit itself. Annual arthropod trapping efforts have collected thousands of specimens representing many different species. Ecogeographical variable layers created in this initiative in consistent spatial coordinate systems and resolutions

can now be applied to these other species, if desired. For example, Noctuidae, *Agrotis* n. sp. caterpillar presence data (n =75) were used to model *Agrotis* species habitat suitability (Figure 23). This model shows that *Agrotis* caterpillars have a greater area of suitable habitat in comparison to wēkiu bugs, presumably because they are a more generalist species and have the ability to burrow into the ash substrate, which wēkiu bugs cannot do (Eiben, Personal Communication, 2015). Jackknife analysis of AUC (Figure 24), percent contribution and permutation importance (Table 6) for *Agrotis* caterpillars reveals that multiple habitat variables, including elevation, aspect, slope, hematite, and amorphous Fe- hydroxide minerals account for large portions of the model, further indicating that this species is more of a generalist and occupies a larger ecological breadth.

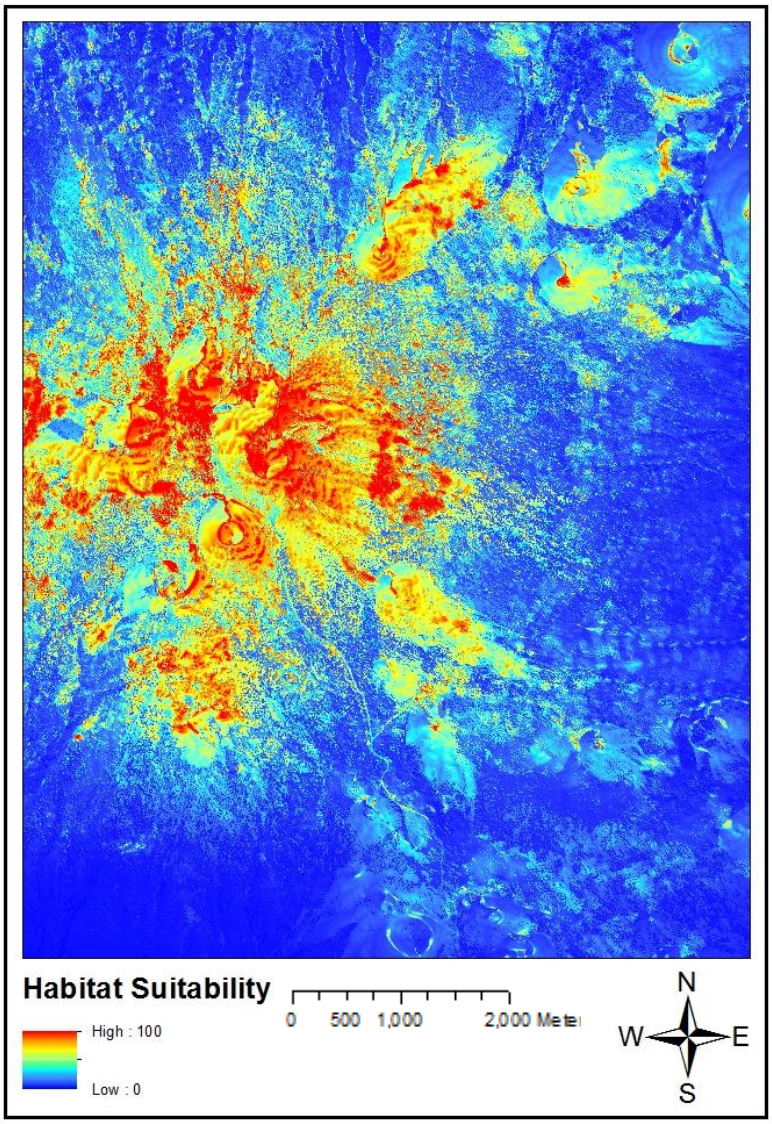

Figure 23: 10 m habitat suitability model highlighting areas of increased suitability (red) and areas unsuitable (blue) for *Agrotis* caterpillars.

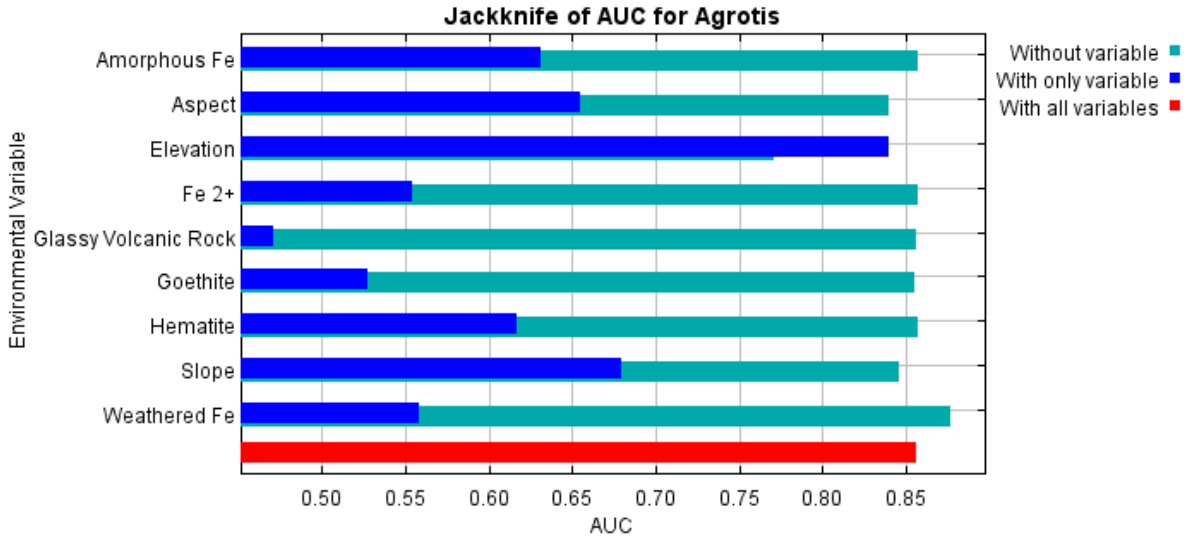

Figure 24: AUC for *Agrotis* caterpillars shows that a number of variables, when run in isolation, account for large portions of the model.

Table 6: Environmental variable importance analysis measured by percent contribution and permutation importance of MaxEnt model for *Agrotis* caterpillars.

Environmental Variable	Percent Contribution	Permutation Importance
Elevation	45.5	45.0
Aspect	10.5	8.0
Slope	14.5	7.5
Hematite	3.4	0.2
Amorphous Fe	13.3	8.0
Weathered Fe	11.9	29.7
Goethite	0.5	1.3
Glassy Volcanic Rock	0.0	0.1
Fe 2+ Minerals	0.3	0.1

Habitat suitability modeling is planned for all endemic, rare or other species of interest on the summit, and once complete we will have a much greater and complete understanding of Maunakea arthropod community dynamics. Models that predict species range within an area can be used to assess species-level interactions, metacommunity structure, evaluate the relative importance of certain traits for an insular ecosystem, and provide insights into biodiversity maintenance and community assemblages (Shipley *et al.* 2012; Stephens & Wiens, 2009; Oke *et al.* 2014; Mihaljevic *et al.* 2015). Competition between species is not directly assessed in these models, but is inherently part of their geographic distributions, which these models can begin to measure (Recart *et al.* 2013; Peers *et al.* 2013).

Maunakea wēkiu bug suitability models may also help predict suitable habitat locations for the much less studied and understood sister species, *Nysius aa* (Polhemus, 1998). *N. aa* is endemic to Mauna Loa, an active shield volcano, with a slightly lower elevation (4170 m) than Maunakea on Hawai‘i Island, with many of the same predominant surface mineral types (Swayze et al. 2002). *N. aa*, much like *N. wekiuicola*, resides in a high elevation desert-type landscape, and presumably fulfills a similar niche scavenging on aeolian deposited insect prey. Species occurrence data for *N. aa* is scant but stored in Bernice Pauahi Bishop Museum collections and results from a single excursion in 2006, which yielded 50 *N. aa* specimens (Englund et al. 2007). Geographic coordinates detailing the limited species occurrence may be used, in conjunction with habitat suitability modeling techniques, to predict where potentially suitable habitat locations are to sample for this additional arthropod species.

CONCLUSION

By integrating a suite of technologies and geospatial techniques with species occurrence data we were able to identify and quantify important habitat metrics and produce overall habitat suitability models for a high altitude Hawaiian species of concern using MaxEnt. This type of approach provides new insights into *Nysius wekiuicola's* spatial patterns on the summit of Maunakea and details important ecogeographical habitat variables that dictate areas of suitability and marginality. This new habitat knowledge and definition will tie directly into conservation management decisions and future habitat restoration efforts on the summit. Annual arthropod trapping campaigns have yielded thousands of specimens over the last fifteen years and the habitat data layers used to model *N. wekiuicola's* habitat can be applied to model geographic ranges and identify important habitat variables for these species as well. Comparing species geographic ranges, occupied ranges, and habitat specificity or generality we can begin to understand arthropod metacommunity dynamics much more thoroughly than in the past.

APPENDICES

All raw data files used in this thesis will be stored in data repositories at Office of Maunakea Management and University of Hawaii at Hilo Spatial Data Analysis and Visualization Lab. For access to these files please contact Nathan Stephenson at nathanms@hawaii.edu.

ASD analysis revealed that each mineral class (Figure 25; Table 7) had distinct spectral signatures. Contrarily, ED XRF revealed that many of the mineral samples had nearly uniform elemental compositions (Figure 10). ASD spectroscopy provides detailed spectral measurements only for the surface (a few microns deep) of a rock sample while ED XRF will provide elemental composition measurements taken from the surface and deeper into the underlying interior rock layers. The base material for the majority of naturally occurring summit rocks is Hawaiite basalt. This explains why many of the mineral samples appear elementally similar. Mineralogy of rocks and rock coatings across the summit may be related to weathering, depositional, sulfuric, or hydrothermal alteration phase changes of Hawaiite basalt lava following emplacement, which may penetrate entire rocks or simply alter a small outer coating (Morris *et al.* 2000; Hon & Swayze, Personal Communication, 2016).

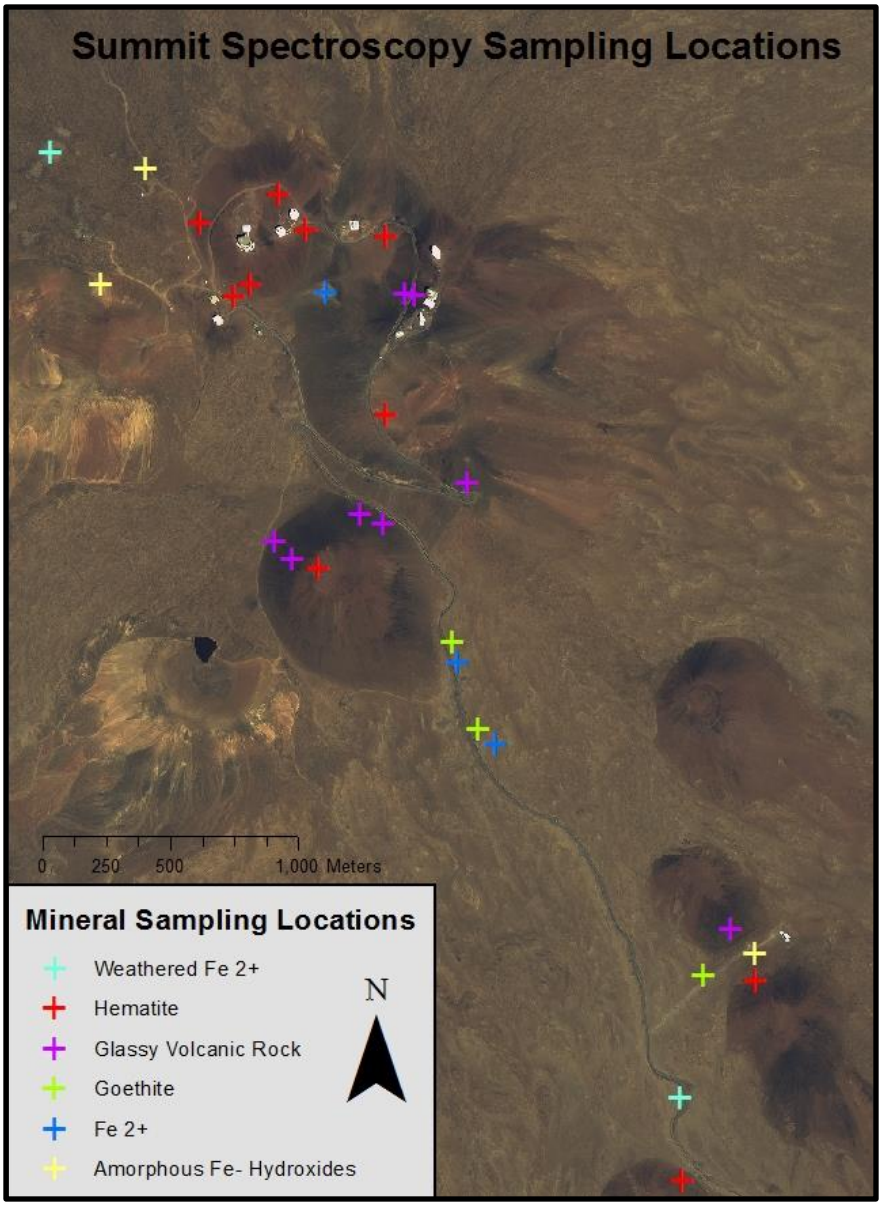

Figure 25: Locations of surface minerals (colored by mineral class) which were analyzed using ASD and ED XRF to determine spectral and chemical characteristics of each mineral type.

Table 7: Locations of surface mineral samples and the mineral class as delineated by the 0.5 m surface mineralogy classification (Figure 6).

Mineral	Northing	Easting
Glassy Volcanic Rock	242540.59	2191410.54
Glassy Volcanic Rock	241182.21	2192990.37
Glassy Volcanic Rock	241091.73	2193030.06
Glassy Volcanic Rock	241514.00	2193153.88
Glassy Volcanic Rock	241307.63	2193882.55
Glassy Volcanic Rock	241267.94	2193890.48
Hematite	242639.01	2191210.78
Hematite	241192.00	2193418.41
Hematite	241192.00	2194112.68
Hematite	240882.97	2194138.08
Hematite	240470.22	2194165.60
Hematite	240599.33	2193879.85
Amorphous Fe- Hydroxides	242638.57	2191315.98
Amorphous Fe- Hydroxides	240252.88	2194374.60
Amorphous Fe- Hydroxides	240081.88	2193928.53
Geothite	242434.13	2191230.76
Geothite	241554.81	2192190.42
Geothite	241454.39	2192528.52
Fe 2+ Minerals	241625.83	2192133.56
Fe 2+ Minerals	241475.06	2192453.28
Fe 2+ Minerals	240960.75	2193895.96
Weathered Fe 2+	242343.63	2190755.07
Weathered Fe 2+	239883.63	2194442.86
Hematite	242353.54	2190430.59
Hematite	240665.65	2193924.41
Hematite	240773.60	2194274.46
Glassy Volcanic Rock	240761.41	2192921.77
Glassy Volcanic Rock	240826.50	2192855.09
Hematite	240929.69	2192815.40

An additional rock sample was collected near an observatory because of its distinct outer alteration sheen and visually different interior layer (Figure 26). Rock sample was analyzed via ASD spectroradiometer. Outer rock coating spectral signature reflected nearly identically to other hematite samples while the interior layer appeared spectrally distinct from all other minerals analyzed (Appendix Figure 3). Although seemingly unrelated to wēkiu bugs, this rock sample highlights the concept that summit rocks may contain an outer mineral coating that is

spectrally different from interior rock layers and helps to explain why ASD results and ED XRF results may differ. This particular rock sample was an olivine xenolith gabbro that was most likely covered in lava as it was emplaced and the Hawaiite basalt lava coating altered into a reddish hematite material but did not penetrate and alter the interior rock layers (Hon, Personal Communication 2016).

Figure 26: Fragment of a much larger rock found near the summit with distinct characteristics including an outer coating that appears to be a different material than the interior layers.

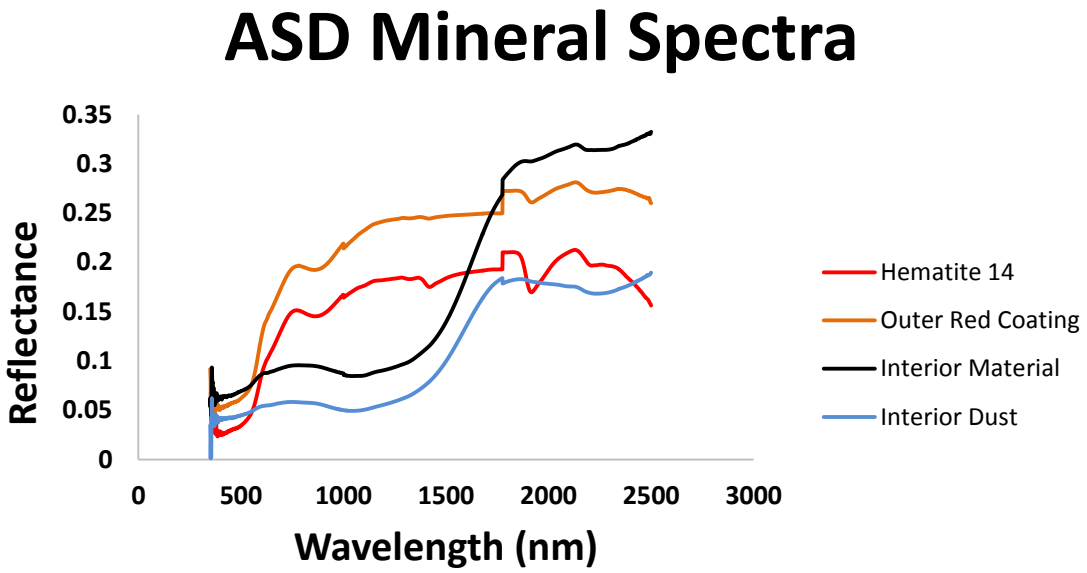

Figure 27: ASD data converted into reflectance for four separate samples. The outer red coating of a unique rock sample (orange) reflects nearly identically to other samples of hematite (red) while the interior material (black) and pulverized interior dust (blue) have a different and unique spectral signature.

Table 8: Locations with depth to the ash layer measurement and associated arthropod trap data.

Northing	Easting	Wekiu Bugs	Depth (cm)		Northing	Easting	Wekiu Bugs	Depth (cm)
240568.2	2193767.19	0	0		240094.05	2193745.79	0	19
240851.92	2193429.84	0	0		240109.7	2193770.14	0	1.2
240831.61	2193552.04	0	0		240231.93	2193804.14	0	3.1
240842.67	2193388.42	0	0		240205.7	2193915.99	11	0.3
240796	2193556.83	0	0		240141.56	2193793.21	0	15.5
240779.29	2193429.37	0	1.2		242713.09	2191412.89	0	0
240759	2193470.97	0	1.2		242444.05	2190497.3	0	6.1
240900.59	2192986.11	19	13.8		242365.32	2190702.89	0	0
240863.47	2193038.05	4	3.9		241499.09	2192374.84	0	7.8
240919.09	2192854.57	11	12.6		240153.19	2194697.74	0	0
240913.68	2192862.88	18	6.8		240195.76	2194555.98	1	0
240926.1	2192835.47	34	6.2		240251.47	2194393.36	0	0
240905.4	2192822.75	5	7.1		240544.97	2193916.81	1	1
240928.79	2192774.89	9	12.9		240476.42	2194003.14	1	3
240914.13	2192753.52	1	0		240491.28	2194009.85	1	0
240990.98	2192704.91	3	9.6		240462.83	2194032.96	0	5
240991	2192725.19	12	0		240435.99	2194105.03	0	0
241066.09	2192744.6	2	9.8		240430.01	2194141.5	0	12
241106.06	2192754.23	5	0		242644.96	2191222.15	4	9.1
240862.16	2192638.03	1	0		242743.97	2191203.95	1	26.2
240812.65	2192564.05	4	0		242749.51	2191178.12	6	0
240662.19	2194251.08	32	1.5		242791.95	2191109.35	1	6.7
240683.64	2194141.08	467	2		242751.33	2191126.93	0	7.8
240647.6	2194115.48	61	1.5		242703.38	2191109.83	0	0.4
240783.18	2194169.71	68	3		241394.02	2193623.76	27	1.5
240772.04	2194156.3	74	0		241339.33	2193580.74	95	1
240755.96	2194189.86	21	3		241309.73	2193508.18	14	3
240711	2194189.48	11	1		241297.2	2193370.68	3	8
240562.58	2194008.97	3	1.5		241256.84	2193361.6	3	7.5
239193.48	2194076.08	0	2.5		241371.64	2193281.77	23	1.5
239148.61	2194032.23	0	0		241481.86	2193347.96	54	1.5
239122.64	2194018.49	0	0		241482.56	2193445.72	0	0
239104.95	2193988.08	0	0		241488.28	2193505.06	3	2
239065.12	2193964.18	0	2.5		241472.25	2193587.03	0	5
238973.26	2193987.32	0	0		240092.33	2193703.85	0	3.5
240254.96	2193896.59	0	9					

REFENCES

Ashlock, P., Gange, W. 1983. A Remarkable New Micropterous Nysius Species from the Aeolian Zone of MaunaKea, Hawai'I Island (Hemiptera: Heteroptera: Lygaeidae). *International Journal of Entomology* 25(1): 47-55.

Asner, G., Knapp, D., Kennedy-Bowdoin, T., Jones, M., Martin, R., Boardman, J. & Hughes, F. 2008. Invasive species detection in Hawaiian rainforests using airborne imaging spectroscopy and LiDAR. *Remote Sensing of Environment* 112: 1942-1955.

Braunisch, V., Coppes, J., Arlettaz, R., Suchant, R., Schmid, R. & Bollmann, K. 2013. Selecting from correlated climate variables: a major source of uncertainty for predicting species distribution under climate change. *Ecography* 36: 971-983.

Brenner, G. 2001-2006. Wēkiu bug Baseline Monitoring. *Pacific Analytics.*

Brenner, G. 2005. Wēkiu Bug Habitat Quantitative Cinder Evaluation. *Pacific Analytics.*

Brown, J. 1984. On the relationship between abundance and distribution of species. *The American Naturalist* 124 (2): 255-279.

Burnet, K., Kaiser, B., Pitafi, B. & Roumasset, J. 2006. Prevention, Eradication, and Containment of Invasive Species: Illustrations from Hawaii. *Agricultural and Resource Economics Review* 35 (1): 63-67.

Cabin, R., Cordell, S., Sandquist, D., Thaxton, J. & Litton, C. 2000. Restoration of tropical dry forests in Hawaii: Can scientific research, habitat restoration, and educational outreach happily co-exist within a small private preserve. *Society for Ecological Restoration* 1-8.

Chen, L., Teo, T., Shao, Y. & Rau, J. 2004. Fusion of Lidar Data and Optical Imagery for Building Modeling. *International Archives of Photogrammetry and Remote Sensing* 35: 732-737.

Costa, G., Nogueira, C., Machado, R., & Colli, G. 2010. Sampling bias and the use of ecological niche modeling in conservation planning: a field evaluation in a biodiversity hotspot. *Biodiversity and Conservation* 19.3: 883-899.

Department of Commerce, National Oceanic and Atmospheric Administration, National Ocean Service, Center for Coastal Monitoring and Assessment, Biogeography Branch. 2007. Digital Elevation Models for the main 8 Hawaiian Islands.

Duman, J. & Montgomery, S. 1991. Subzero temperature adaptations in arthropods from the summit of Mauna Kea, Hawaii. *Journal of Experimental Zoology* 259: 409-412.

Eiben. 2015. Personal Communication. Moth captive rearing and species identification.

Eiben, J., Rubinoff, D. 2010. Life history and captive rearing of the Wēkiu bug (*Nysius Wēkiuicola,* Lygacidae), an alpine carnivore endemic to the Mauna Kea volcano of Hawaii. *Insect Conservation* 14: 701-709.

Eiben, J., Rubinoff, D. 2014. Application of Agriculture-Developed Demographic Analysis for te Conservation of the Hawaiian Alpine Wekiu Bug. *Conservation Biology* 28(4): 1077-1088.

Elith, J., Graham, C., Anderson,R., Dudik, M., Ferrier, S., Guisan, A., Hijmans, R., Huettmann, F., Leathwick, J., Lehmann, A., Li, J., Lohmann, L., Loiselle, B., Manion, G., Moritz, C., Nakamura, M., Nakazawa, Y., Overton, J., Peterson, A., Phillips, S., Richardson, K., Scachetti-Pereira, R., Schapire, R., Soberon, J., Williams, S., Wisz, W. & Zimmermann, N. 2006. Novel methods improve prediction of species' distributions from occurrence data. *Ecography* 29: 129-151.

Elith, J., Phillips, S., Hastie, T., Dudik, M, Chee, Y. & Yates, C. 2010. A statistical explanation of MaxEnt for ecologist. *Wiley Online Library.*

Englund, R., Vorsino, A. & Laederich, H. 2007. Results of the 2006 Wēkiu bug (Nysius wekiuicola) surveys on Mauna Kea, Hawai'i Island. *Bishop Museum.*

Englund, R., Preston, S., Englund, L., Imada, C., Evenhuis, N. Results of the 2007-2008 (2009,2010,2011,2012,2013) Alien Species and wēkiu bug (Nysisu Wekiuicola) Surveys on the Summit of Mauna Kea, Hawai'i Island. *Bishop Museum.*

Franklin, J., Wejnert, K., Hathaway, S., Rochester, C. & Fisher, R. 2009. Effects of species rarity on the accuracy of species distribution models for reptiles and amphibians in southern California. *Diversity and Distributions* 15: 167-177.

Franklin, J. 2010. Mapping Species Distributions: Spatial Inference and Prediction. *Cambridge University Press.*

Franklin, J. Davis, F., Ikegami, M., Syphard, A., Flint, L., Flint, A. & Hannah, L. 2012. Modeling plant species distributions under future climates, how fine scale do climate projections need to be? *Global Change Biology* 19.2: 473-483.

Giambelluca, T.W., X. Shuai, M.L. Barnes, R.J. Alliss, R.J. Longman, T. Miura, Q. Chen, A.G. Frazier, R.G. Mudd, L. Cuo, and A.D. Businger. 2014. Evapotranspiration of Hawai'i. Final report submitted to the U.S. Army Corps of Engineers—Honolulu District, and the Commission on Water Resource Management, State of Hawai'i.

Giambelluca, T.W., Q. Chen, A.G. Frazier, J.P. Price, Y.-L. Chen, P.-S. Chu, J.K. Eischeid, and D.M. Delparte, 2013: Online Rainfall Atlas of Hawai'i. Bull. Amer. Meteor. Soc. 94, 313-316, doi: 10.1175/BAMS-D-11-00228.1.

Guinness, E. A., Arvidson, R. E., Jolliff, B. L., Seelos, K. D., Seelos, F. P., Ming, D. W., Morris, R. V. & Graff, T. G. 2007. Hyperspectral reflectance mapping of cinder cones at the summit of Mauna Kea and implications for equivalent observations on Mars. *Journal of Geophysical Research* 112: E08S11.

Hannam, M. & Moskal. M. 2015. Terrestrial Laser Scanning Reveals Seagrass Microhabitat Structure on a Tideflat. *Remote Sensing* 7 (3): 3037-3055.

Hernandez, P., Graham, C., Master, L. & Albert, D. 2006. The effect of sample size and species characteristics on performance of different species distribution modeling methods. *Ecography* 29: 773-785.

Hirzel, A., Hauseer, J., Chessel, D. & Perrin, N. Ecological-Niche Factor Analysis: How to Compute Habitat-Suitability Maps Without Absence Data? *Ecology* 83 (7): 2027-2036.

Hon, Ken. 2016. Personal Communication – Petrology of rock samples, ASD & ED XRF results.

Howarth, F., Montgomery, S. 1980. Notes on the ecology of the high altitude Aeloian zone on Mauna Kea. *Elepaio* 41(3): 259-264.

Isik, K. 2011. Rare and endemic species: why are they prone to extinction? *Turkish Journal of Botany* 35 (4): 411-417.

Juvik, J. & Juvik S. 1984. Mauna Kea and the Myth of Multiple Use Endangered Species and Mountain Management in Hawaii. *Mountain Research and Development* 4 (3): 191-202.

Kadmon, R., Farber, O. & Danin, A. 2004. Effect of roadside bias on the accuracy of predictive maps produced by bioclimatic models. *Ecological Applications* 14 (2): 401-413.

Kirkpatrick, J. & Klasner, F. 2015. Standard Operating Procedure C:Maunakea Invertebrate Threats, Identification, Collection, and Processing Guide.

Kramer-Schadt, S., Niedballa, J., Pilgrim, J., Schroder, B., Lindenborn, J., Reinfelder, V., Stillfired, M., Heckman, I., Scharf, A., Augeri, D., Cheyne, S., Hearn, A., Ross, J., Macdonald, D., Mathai, J., Eaton, J., Marshall, A., Semiandi, G., Rustam, R., Bernard, H., Alfred, R., Samejima, H, Duckworth, J., Breitenmoser-Wuersten, C., Belant, J., Hofer, H. & Wilting, A. 2013. The importance of correcting for sampling bias in MaxEnt species distribution models. *Diversity and Distributions* 19: 1366-1379.

Kruckeberg, A. & Rabinowitz, D. 1985. Biological Aspects of Endemism in Higher Plants. *Annual Review of Ecology and Systematics* 447-479.

Kumar, S. & Stohlgren, T. 2009. Maxent modeling for predicting suitable habitat for threatened and endangered tree *Canacomyrica monticola* in New Caledonia. *Journal of Ecology and Natural Environment* 1 (4): 094-098.

Leslar, M. 2015. Integrating Terrestrial Lidar with Point Clouds Created From Unmanned Aerial Vehicle Imagery. *The International Archives of the Photogrammetry, Remote Sensing and Spatial Information Sciences* Volume XL-1/W4.

Loarie, S., Carter, B., Hayhoe, K., McMahon, S., Moe, S., Knight, C. & Ackely, D. 2008. Climate Change and the Future of California's Endemic Flora. *PLoS ONE* 3 (6).

Lundblad, S. P., P. R. Mills and K. Hon. 2008. Analysing Archaeological Basalt Using Non-destructive Energy-dispersive X-ray Fluorescence: effects of post-depositional chemical weathering and sample size on analytical precision. Archaeometry 50(1):1-11.

Lundblad, S.P., P.R. Mills, A. Drake-Raue, and S.K. Kikiloi. 2011. Non-destructive EDXRF analyses of archaeological basalts. in M.S. Shackley (ed.) X-ray fluorescence Spectrometry in Geoarchaeology. New York, Springer Press. 65-80.

Magris, F. & Destro, G. 2010. Predictive modeling of suitable habitats for threatened marine invertebrates and implications for conservation assessment in Brazil. *Brazilian Journal of Oceanography*: 1982-436X.

Manthey, J., Campbell, L., Saupe, E., Soberon, J, Hensz, C., Myers, C., Owens, H., Ingenloff, K., Peterson, A., Barve, N., Lira-Noriega, A. & Barve, V. 2015. A test of niche centrality as a determinant of population trends and conservation status in threatened and endangered North American birds. *Endangered Species Research* 26: 201-208.

McCoy, P. 1976. The Mauna Kea Adze Quarry Complex, Hawaii: A First Analysis. *Proceedings of the First Conference on Natural Sciences in Hawaii. Cooperative National Park Resources Studies Unit, University of Hawaii.*

Merow, C., Smith, M. & Silander, J. 2013. A practical guide to MaxEnt for modeling species' distributions: what it does, and why inputs and settings matter. *Ecography*36: 1058-1069.

Mihaljevic, J., Joseph, M. & Johnson, P. 2015. Using multispecies occupancy models to improve the characterization and understanding of metacommunity structure. *Ecology* 96 (7): 1783-1792.

Morris, R., Golden, D., Bell, J., Shelfer, T., Scheinost, A., Hinman, N., Furniss, G., Mertzman, S., Bishop, J., Ming, D., Allen, C. & Britt, A. 2000. Mineralogy, composition, and alteration of Mars Pathfinder rocks and soils: Evidence from multispectral, elemental, and magnetic data on terrestrial analogue, SNC meteorite, and Pathfinder samples. *Journal of Geophysical Research* 105: 1757-1817.

Office of Maunakea Management. 2009. Natural Resources Management Plan for the UH Management Areas on Mauna Kea. *Sustainable Resources Group Intn'l, Inc.*

Office of Maunakea Management. 2014-2015. Annual alien arthropod and wēkiu bug (Nysius wekiuicola) survey results for Mauna Kea.

Okal, M. 2016. Mauna Kea Erosion, Mauna Kea, Hawaii. UNAVCO Inc.

Oke, O., Heard, S. & Lundholm, J. 2014. Integrating phylogenetic community structure with species distribution models: an example with plants of rock barrens. *Ecography* 37: 001-012.

Peers, M., Thornton, D. & Murrary, D. 2013. Evidence for large-scale effects of competition: niche displacement in Canada lynx and bobcat. *Proceedings of the Royal Society of London B: Biological Sciences* 280.1773: 1-10.

Peterson, A. & Nakazawa, Y. 2008. Environmental data sets matter in ecological niche modelling: an example with *Solenopsis invicta* and *Solenopsis richteri*. *Global Ecology and Biogeography* 17: 135-144.

Perroy, R., Bookhagen, B., Asner, P. & Chadwick, O. 2010. Comparison of gully erosion estimates using airborne and ground-based LiDAR on Santa Cruz Island, California. *Geomorphology* 118 (3): 288-300.

Phillips, S., Anderson, R. & Schapire, R. 2006. Maximum entropy modeling of species geographic distributions. *Ecological Modelling* 190: 231-259.

Phillips, S. & Dudik, M. 2007. Modeling of species distributions with Maxent: new extensions and a comprehensive evaluation. *Ecography* 31 (2): 161-175.

Phillips, S., Dudik, M., Elith, J., Graham, C., Lehmann, A., Leathwick, J. & Ferrier, S. 2009. Sample selection bias and presence-only distribution models: implications for background and pseudo-absence data. *Ecological Applications* 19 (1): 181-197.

Polhemus, D. 1998. *Nysius AA* (Heteroptera: Lygaeidae), A New Species of Micropterous Wekiu Bug from the Summit of Mauna Loa Volcano, Hawaii. *Proceedings of the Entomological Society of Washington* 100 (1): 25-31.

Porter, S. 2005. Pleistocene snowlines and glaciation of the Hawaiian Islands. *Quaternary International 138-139: 118-128.*

Porter, S., Englund R. 2006. Possible geologic factors influencing the distribution of the Wekiu Bug on Mauna Kea, Hawaii. Final Rep prep Office of Mauna Kea Management, Hilo, Hawaii, 29 pp.

Rabinowitz, D. 1981. Seven forms of rarity. The Biological Aspects of Rare Plant Conservation. 205-217.

Rapidlasso. 2015. LAStools: Award-winning software for efficient LiDAR processing.

Razgour, O., Hanmer, J. & Jones, G. 2011. Using multi-scale modelling to predict habitat suitability for species of conservation concern: The grey long-eared bat as a case study. *Biological Conservation*: doi:10.1016/j.biocon.2011.08.010.

Recart, W., Ackerman, J. & Cuevaas, A. 2013. There goes the neighborhood: apparent competition between invasive and native orchids mediated by a specialist florivorous weevil. *Biological Invasions* 15.2: 283-293.

Reed, J., Desrochers, D., Vanderwerf, E. & Scott, M. 2012. Long-Term Persistence of Hawaii's Endangered Avifauna through Conservation- Reliant Management. *BioScience* 62 (10): 881-892.

Rhee, S. & Kim, T. 2015. Automated DSM extraction from UAV images and Performance Analysis. *The International Archives of Photogrammetry, Remote Sensing and Spatial Information Sciences* 41.1: 351-356.

Ribeiro, K. & Fernandes, W. 2000. Patterns of Abundance of a Narrow Endemic Species in Tropical and Infertile Montane Habitat. *Plant Ecology* 147 (2): 205-218.

Richards, J.A., 1999, Remote Sensing Digital Image Analysis, Springer-Verlag, Berlin, p. 240.

Richardson, M. 2002. Life in Mauna Kea's Alpine Desert. *Endangered Species Bulletin* 27(2): 22-23.

Rochlin, I., Ninivaggi, D., Hutchinson, M. & Farajollahi, A. 2013. Climate Change and Range Expansion of the Asian Tiger Mosquito (*Aedes albopictus*) in Northeastern USA: Implications for Public Health Practitioners. *PLoS ONE* 8 (4): 1-7.

Segurado, P. & Araujo, M. 2004. An evaluation of methods for modelling species distributions. *Journal of Biogeography* 31: 1555-1568.

Shipley, B., Paine, C. & Baraloto, C., 2012. Quantifying the importance of local niche-based and stochastic processes to tropical tree community assembly. *Ecology* 93 (4): 760-769.

Silva, S. & Businger, S. 2006. Climatological Analysis of Meteorological Observations at the Summit of Mauna Kea. *Faculty of Sciences University of Lisbon, Physics Department.*

Stemmermann, L. 1989. Rare Plants and the Federal Endangered Species Act. *Conservation Biology in Hawaii Cooperative National Park Resources Studies Unit, University of Hawaii Press, Honolulu* 48-54.

Stephens, P. & Wiens, J. 2009. Bridging the gap between community ecology and historical biogeography: niche conservatism and community structure in emydid turtles. *Molecular Ecology* 18: 4664-4679.

Swayze, G. 2016. Personal Communication. ASD & ED XRF results.

Swayze, G., Clark, R., Sutley, S., Gent, S., Rockwell, B., Blaney, D., Post, J. & Farm, P. 2002. Mineral Mapping Mauna Kea and Mauna Loa Shield Volcanos on Hawaii Using AVIRIS Data and the USGS Tetracorder Spectral Identification System: Lessons Applicable to the Search for relict Martian Hydrothermal Systems. *Proceedings of the 11th JPL Airborne Earth Science Workshop, JPL Publication3-4.*

Syfert, M., Smith, M. & Coomes, D. 2013. The effects of Sampling Bias and Model Complexity on the Predictive Performance of MaxEnt Species Distribution Models. *PLoS ONE* 8 (2): 1-10.

Thirty Meter Telescope Final Environmental Impact Statement. 2010.

Thuiller, W. & Munkemuller, T. 2010. Habitat suitability modelling. *Oxford University Press, New York.* 77-85.

Vaughan, I. & Omerod, S. 2003. Improving the Quality of Distribution Models for Conservation by Addressing Shortcomings in the Field Collection of Training Data. *Conservation Biology* 17 (6): 1601-1611.

Wolfe, W. & Morris, J. 1996. Geologic Map of the Island of Hawaii. *U.S. Geological Survey*.

Weinsheimer, F., Mengistu, A. & Rodder, D. 2010. Potential distribution of threatened Leptopelis spp. (Anura, Arthroleptidae) in Ethiopia derived from climate and land-cover data. *Endangered Species Research* 9:117-124.

Wiens, J., Stralberg, D., Jongsomjit, D., Howell, C. & Synder, M. 2009. Niches, models, and climate change: Assessing the assumptions and uncertainties. *Proceedings of the National Academy of Sciences of the United States of America* 106 (2): 19729-19736.

Wood, R. & Mohammadi, M. LiDAR Scanning with Supplementary UAV Captured Images for Structural Inspections.

Wolfe, E. W., Wise, W. S. & Dalrymple, G. B., 1997. The geology and petrology of Mauna Kea volcano, Hawaii: a study of post shield volcanism. *U. S. Geological Survey Professional Paper* 1557, 129 p.

Young, N., Carter, L. & Evangelista, P. 2011. A MaxEnt Model v3.3.3e Tutorial (ArcGIS v10). Natural Resource Ecology Laboratory at Colorado State University and the National Institute of Invasive Species Science.